Effect of ultraviolet radiation on phytoplankton photosynthesis measured using fiber-optical oxygen sensors.

Master's thesis in optical and atomic physics

By

Ssenyunzi Richard Cliffe

University of Bergen, Norway
Department of physics and technology

December 2009

Contents

Acknowledgement 4

LIST OF ABBREVIATIONS 5

ABSTRACT 7

1 Introduction 8

1.1 Penetration of UV in the aquatic ecosystem 9

1.2 Phytoplankton 10

1.3 Aim of the thesis 13

2. Theory 14

2.1 PHOTOSYNTHESIS 14

2.2 Photosynthetic pigments 14

2.3 Light and dark reactions 17

2.4 The principles of photosynthesis 18

2.5 Photosynthetic oxygen formation 21

2.6 Effects of UVR on photosynthesis 22

2.6.1 Direct effects 23

2.6.2 Indirect effects 24

2.7 Mechanism to reduce the effects of UVR on photosynthesis 24

3 The principle of the 10-channel Fiber-Optic Oxygen Meter (oxy-10) 27

3.1 The oxy-10 meter 27

3.1.1 The fiber optical micro sensor 28

3.2 Spectroscopic principles of optical sensing 29

3.2.1 Principle of the fiber optical micro sensor 31

4 MATERIAL AND METHODS 34

4.1 LABORATORY EXPERIMENTS 34

4.1.1 An experimental system (Photoinhibitron) for testing the effects of UVR on phytoplankton 34

4.1.2 Irradiance measurements 39

4.1.3 Cultures 40

4.1.4 Measurements of photosynthesis (oxygen measurements) 41

4.1.5 Calibration of the fiber optical micro sensors 43

5 Results and discussions 45
5.1 Variation of photosynthetic rate with irradiance 45
5.2 The effect of UVR on algae photosynthesis 47
5.2.1 Inhibition of photosynthesis in *Haematococcus pluvialis* (green algae) 48
5.2.2 Methodical problems 50
5.2.3 Inhibition of photosynthesis in *Phaeodactylum tricornutum* (diatom 53
6 Conclusion and further research. 59
References 61

Acknowledgement

The completion of this thesis marks the final input to accomplish a master's program in Physics. This program is a product of the dedicated efforts and wisdom of the department of Physics and Technology of the University of Bergen (UiB). For this reason I pay my respect to all the staff that made this great program a reality.

In a special way I extend my sincere gratitude to my supervisors, Øyvind Frette (Department of physics and technology) and Svein Rune Erga (Department of Microbiology), your guidance, experience and counsel throughout the entire year of research have been so invaluable. I am also grateful to the mechanical work shop staff for the assistance in the construction of the experimental system.

I would like to thank Lånekassen through the student services at UiB for finding and facilitating my master's studies. It is highly probable that without your support I may not have been able to pursue my dream. I would also like to thank all my classmates who have supported, encouraged and provided me with kind and helpful advices.

Very special thanks go to my brother Ssebiyonga Nicolausi for his endless helping during the entire research period. I also appreciate the great help by friends Olowo and Wandela for proof reading my work.

Words fail to express the appreciation I have for my dear friend, Nanyiti Julian's support. She encouraged me to follow my dreams and take this path and was my foundation throughout. She has my utmost respect and admiration and, of course my deepest love.

To my parents, Sarah Nammuli and Daniel Kaggwa, your hard work and love for me have defined my success.

Lastly, I thank the almighty God, you have been my strength and constant provider, you have blessed me so much in this journey.

Bergen, December 6, 2009

Ssenyunzi Richard Cliffe.

LIST OF ABBREVIATIONS

nm	nanometer
PAR	photosynthetically available radiation (400-700 nm)
P	PAR
PA	PAR+UV-A
PAB	PAR+UV-A+UV-B
PAM	pulse-amplitude modulation
PS-I	photosystem I
PS-II	photosystem II
UVR	ultraviolet radiation
UV-A	ultraviolet-A (320-400 nm)
UV-B	ultraviolet-B (280-320 nm)
UV-C	ultraviolet-C (100-280 nm)
λ	wavelength (nm)
ATP	adenosine triphosphate.
	End product of light reaction
LED	light emitting diode
LHCI, LHCII	light harvesting complexes.
	Responsible for the absorption of light in PS-I and PS-II
NADP	nicotinamide adenine dinucleotide phosphate.
	End product of light reaction
P700	chlorophyll *a* molecule absorbing light in PS-I at 700 nm
P680	chlorophyll *a* molecule absorbing light in PS-II at 680 nm
PMT	photomultiplier tube.
	Photon detector
P_{inh}	photosynthesis in exposed samples relative control
P_{UVR}	photosynthesis after UV-B radiation treatment
P_{PAR}	uninhibited photosynthesis
O_2	oxygen
H_2O	water

H^+	hydrogen ion
DOM	dissolved organic matter
PC	plastocyanin. Copper-containing protein
Q_A and Q_B	plastoquinone molecules. Transporting electrons from PS-II to PS-I
NADPH	the reduced form of nicotinamide adenine dinucleotide phosphate
Pi	phosphate ion
ADP	adenosine disphosphate
Fd	ferredoxine
OEC	oxygen evolving complex (attached to PS-II)
BWF	biological weighting function
DNA	deoxyribonucleic acid
MAA	mycosporine-like amino acid
RubsiCO	Ribulose-1,5-bisphosphate carboxylase oxygenase

ABSTRACT

Since the discovery of the Antarctic ozone 'hole' many studies have been conducted to determine the effect of UV radiation on photosynthetic rate of phytoplankton. It is accepted now that increased levels of UV radiation are stressful for some phytoplankton. In this thesis have developed and implemented an experimental system (a photoinbitron) for measuring photosynthesis of phytoplankton suspensions during controlled, quantified exposures to a broad range of UV radiation and PAR treatments. We have also carried out experiments to evaluate the effects of UVR on phytoplankton photosynthesis. The results from this experiment presented two selected algae species from different classes, *Haematococcus pluvialis* and *Phaeodactylum tricornutum* which differ in many ways, especially in regard to their habitats. The impact of UVR was assessed by exposing the samples to a constant irradiance of UVA and PAR but with varying irradiances of UVB exposure which ranged from 20% to 100% of the maximum available intensity. The radiation was divided into five different radiation treatments using cut off filters (280, 295, 305 and 395) so that samples received radiation at five different intervals within the UVR in addition to PAR, and only PAR respectively.

For irradiation treatment (PAR) without UVR, photosynthesis in all samples tested was not affected during the course of 20 min of exposure. When the samples were exposed to full irradiance spectra, photosynthesis was inhibited to a variable degree in all samples of the two algae species tested. Strong inhibition was observed in algae samples when the UVB levels were at 100% and least inhibition when levels of UVB exposure were at 20%. Of the two selected species tested, the most sensitive specie was *Phaeodactylum tricornutum* and *Haematococcus pluvialis* was the least sensitive to UVB irradiance. This may probably be related to adaptation through the accumulation of UVB screening compounds, to high UVB levels. Most of the observed variability in all the samples tested was due to change in UVB levels. Photosynthetic oxygen evolution performances in response to UVB were measured using oxygen fiber optical micro sensors which are based on oxygen dependent dynamic fluorescence quenching.

.

1 Introduction

Solar radiation is a prerequisite for life on Earth and is emitted as electromagnetic radiation over a wide range of wavelengths. The maximum intensity in the solar emission spectrum is around 500 nm which is in the blue-green part of the visible spectrum. The visible light which covers the wavelength rage 400-700 nm is referred to as the Photosynthetically Active Radiation (PAR).

As well as a visible light the sun emits the more energetic ultra violet radiation Ultraviolet Radiation (UVR) can be defined as the part of the solar spectrum with wavelengths below 400 nm. UVR that reaches the Earth's surface is in the wavelength range between 280 and 400 nm and has a potential of affecting organisms negatively.

The solar radiation measured at the Earth's surface is subjected to atmospheric absorption and scattering by gas molecules, aerosols, and clouds. The UVR (200-400nm) can be sub-divided into UV-A (400 nm-320 nm), UV-B (320 nm-280 nm) and UV-C (280 nm-200 nm) [1]. Although the UV radiation has the high photon-specific energy, it only makes up a small portion of around 6% of the solar energy reaching the surface of the Earth.

The world is protected from an excess amount of UV radiation by the ozone layer found in the stratosphere which is located 20-40 km above the Earth's surface. The ozone layer filters the potentially damaging part of the radiation from reaching the Earth's surface. The highest percentage of the UV radiation (about 90%) reaching the Earth's surface is the UV-A which has the longest wavelengths. UV-A radiation is relatively weakly affected by variations in stratospheric ozone concentrations, and it is the least damaging form of UV radiation. The other UV radiation that also reaches the Earth's surface is UV-B which can be highly damaging to organisms. This type of radiation increases most significantly when stratospheric ozone is reduced. The shortest and the most harmful UV wavelengths is the UV-C. These wavelengths are strongly absorbed by the ozone in the stratosphere so that negligible amounts reach the Earth's surface.

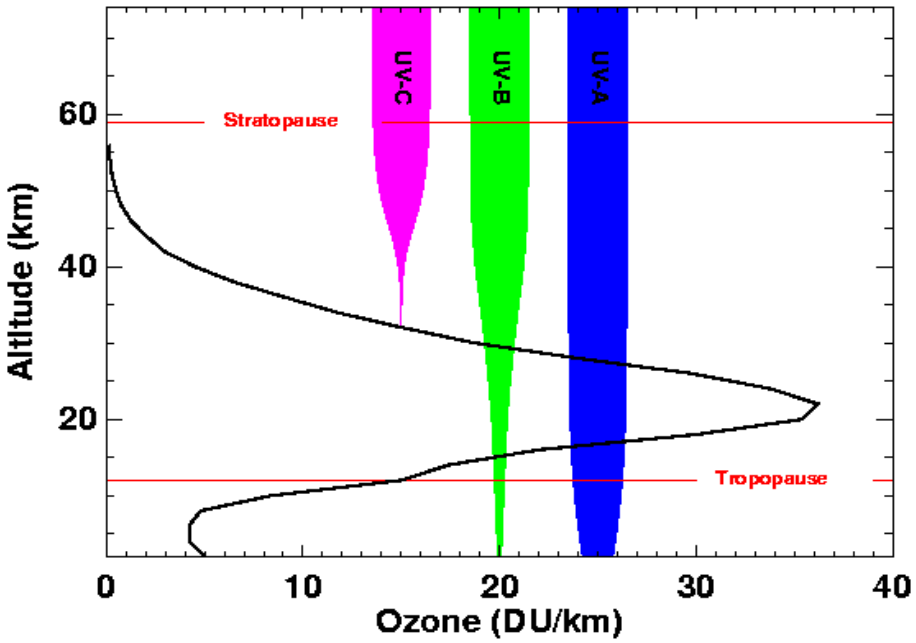

Figure: 1.1-The figure shows a vertical profile of midltitude ozone: the concentration of ozone as a function of altitude. On the figure are also plots of UVR as a function of altitude for UV-A (blue), UV-B (green), and UV-C (red). Figure adapted from Stratospheric Ozone. An Electronic Textbook [2]

Figure 1.1 shows how far into the atmosphere each of the three types of UV radiations penetrates. UV-C is completely absorbed by ozone at around 35 km altitude, most of UV-B is absorbed by ozone, but some reaches the surface and most of UV-A reaches the surface.

1.1 Penetration of UV in the aquatic ecosystem

UVR can penetrate into water bodies to a considerable depths [3] its penetration has a significant ecological impact in the marine environment [4], and it is strongly influencing biological productivity. The UVR penetration into water depends not only on the atmospheric conditions such as latitude and altitude, sun elevation due to season and time of the day, cloud cover, ozone concentration, but also depends on the optical properties of the water body [5] [6]. The effects of UV radiation on the marine ecosystem have been given attention by scientists since the depletion of stratospheric ozone was observed in Antarctica in the early 1980's [7]. This has led to a significant global concern about the

increased exposure of the aquatic ecosystem to damaging UV radiation. In Antarctic oceanic waters, detectable levels of UV-B were recorded to a depth of 60-70 m [8]. In coastal waters, UV-B reaches only to 1 m depth, as in the Baltic Sea [9]. This variability depends mostly on the concentration of chlorophyll *a* and the dissolved organic matter (DOM) [5] present in the water body.

The main area of interest in the study of the impact of UV radiation on the aquatic ecosystem is the phytoplankton. UV radiation has damaging effects on marine phytoplankton [10] [11] and this is shown in marine phytoplankton in Antarctica which are UV stressed [12]. Therefore UV radiation should be considered a very important environmental factor that can affect different metabolic and physiological processes in autotrophic organisms living in water.

1.2 Phytoplankton

Phytoplankton are unicellular, microscopic plants that populate the top layers of oceans and freshwater habitats where they receive sufficient solar radiation for photosynthetic processes. This layer is called the euphotic zone [13] [14]. Within this zone, phytoplankton are simultaneously exposed to solar UV-radiation, in addition to the longer-wavelength radiation (PAR). The increase in the amount of UV radiation which penetrates the euphotic zone has affected the phytoplankton productivity. Phytoplankton live in an environment where factors such as availability of light, uptake of nutrients, sinking and grazing pressure affect their growth, and distribution [15].

Recent studies about aquatic ecosystems, have led to an agreement that environmental UV-B, independent of ozone related increases, is an ecological stress that influences the growth, survival, and distribution of phytoplankton. On the global scale, phytoplankton are the most important primary producer in the aquatic food web [11] [14], they serve the primary consumers as food, which are in turn consumed by secondary consumers. Therefore any decrease in their productivity or population may have significant consequences on the intricate food web in the aquatic ecosystems and affect food productivity. The human population may also be affected by consequences of increased

UV radiation on the aquatic food web. This is because more than 30% of the global animal proteins for human consumption come from the sea and oceans, a substantial decrease in biomass production would significantly affect the global food supply. In addition, the decrease in phytoplankton growth is related to the reduction of the carbon uptake [16]. The ability of the oceans to act as atmospheric carbon sink is reduced when there is a reduction in the marine phytoplankton productivity. Phytoplankton which are said to produce over a half of the global biomass, also absorb and fix over a half of the carbon from the atmosphere. It is estimated that for a loss of about 10% of marine phytoplankton, about 5Gt of carbon would be prevented from being removed from the atmosphere annually [17]. Since carbon dioxide is the most important green house gas, any reduction in carbon uptake would have implications on global warming scenarios.

Phytoplankton have the ability to transform the energy from the sun together with nutrients in water, into carbohydrates through a process called photosynthesis. Through this process the phytoplankton are responsible for producing over 50% of the oxygen present in the atmosphere of our planet. Therefore any factor that affects the process of photosynthesis will lead to reduction in oxygen.

Phytoplankton through photosynthesis, give rise to fossil fuels which play a very important part in the world's economy. Organic carbon from primary production is stored in organisms and when these organisms die they sink to the ocean floor and get buried in the sediments and mud at the bottom of the oceans. The different pressures and temperatures under the ocean floor act on these dead organisms and lead to the formation of hydrocarbons from which oils and gas are developed.

Ecological studies on the impact of UV radiation on phytoplankton need to carefully quantify the UV exposure whether working in the laboratory or in the field. In these studies it's important to consider both the quantity (energy content of UV) and the quality (energy spectral composition which shows energy at each wavelength) of UV radiation because the potential damage caused by UV radiation is heavily wavelength dependent [18].

In nature there are tremendous changes in spectral composition of UV as a function of the season, latitude, time of the day, atmospheric conditions and so on. In the aquatic environment the spectral composition of UV radiation may be further modified by the dissolved and particulate substances in the water which show strong variations in space and time One way of changing the UV range of spectra is by use different cut-off filters and thus a variety of proportions between PAR and UVR can be studied. With artificial lights and algae cultures, measurements in laboratory can give a picture of the possible variability in response to UVR which describe the effectiveness of different wavelengths to produce biological responses.

Photosynthesis, a process that takes place in phytoplankton is the biggest contributor of the total primary production in the oceans. In oceans, almost all primary production is performed by microscopic organisms, the phytoplankton. In phytoplankton community, primary production is performed by both microscopic algae and the cyanobacteria (photosynthetic bacteria). Primary production refers to the formation of organic compounds from atmospheric or aquatic carbon dioxide by autotrophs (primary producers) using sunlight as the main source of energy. The major regulators of primary production in the ocean are light, turbulent motions, availability of nutrients, temperature [19] [20] and any other factor that inhibits photosynthesis.

Studies on the effect of UVR upon phytoplankton photosynthesis have been conducted using both natural communities and monospecific cultures [21] [22]. The exposure of samples has included *in situ* experiments [23] as well as the use of laboratory experiments.

Various experimental approaches have been used to evaluate primary production as well as the impact of UVR on different phytoplankton processes. The evolution of oxygen [24] and incorporation of radiocarbon (C-14) [25] have been widely used not only to determine primary production, but also to asses the impact of UVR [26]. In addition, oxygen micro sensors [27] have been shown to be practical tools for higher-resolution measurements of UVR effects in sediments and microfilms [28] [29], particularly in

combination with optical micro sensors measuring UVR [30]. But also in recent years, pulse amplitude modulated (PAM) chlorophyll fluorescence associated with the photo system II (PSII) has become a useful tool for evaluation of photosynthesis [31] [32]. Chlorophyll fluorescence can function as an indicator of different functional levels in photosynthesis, such as photon capture by light harvesting pigments, primary light reaction, thylakoid electron transport reactions, dark-enzymatic stroma reactions, and slow regulatory feedback processes [33]. The relationship between oxygen evolution and chlorophyll fluorescence in different organisms has also been investigated [34] [35].

Photosynthetic activity has been estimated as oxygen evolution using fiber optical oxygen sensors in phytoplankton, macroalgae and cynobacteria [36] [37]. This technique of using fiber optical oxygen sensors is advantageous for long term measurements, as it does not consume oxygen itself. Therefore we decided to use this technique to quantify photosynthetic oxygen evolution during our experiments in investigating the effect of UVR on phytoplankton photosynthesis.

1.3 Aim of the thesis

The aim of this thesis was to developed an experimental system (photoinhibitron) and use it to investigate the role of UVR in affecting the photosynthetic process in the micro algae based on laboratory studies with selected species. This is especially important as the effects of UVR on photosynthesis of micro algae may have a considerable impact on higher trophic levels of aquatic ecosystem [38] as well as in climate change [39].

We measured photosynthesis of phytoplankton suspension during controlled, quantified exposure to PAR and UVR using the fiber optical micro oxygen sensors as the oxygen evolution (photosynthesis) measurement technique.

2. Theory

2.1 PHOTOSYNTHESIS

Photosynthesis describes the process by which plants, algae and photosynthetic bacteria synthesize organic compounds from inorganic raw materials (water and carbon dioxide) by utilizing light energy. The overall process of photosynthesis is represented by Equation 2.0.

$$6CO_2 + 6H_2O \xrightarrow{\text{light energy}} C_6H_{12}O_6 + 6O_2$$

The carbohydrates formed in the process have more energy than the raw materials which are carbon dioxide and water.

The rate of photosynthesis is affected by a number of factors which include light levels, temperature, and availability of nutrients, availability of carbon dioxide, salinity, pressure and biological effects [40] [41].

2.2 Photosynthetic pigments

Pigments are molecules with particular characteristic absorption spectra in response to light. They are found in the chloroplasts and are located in the thylakoid membranes. The color of the pigment depends upon the wavelengths of light that are absorbed. Since pigments interact with light to absorb only certain wavelengths, they are very important to plants and other autrophs organisms for photosynthesis.

In plants, algae, and cyanobacteria, pigments are responsible for the harvesting of the light energy needed for photosynthesis. However, since each pigment absorbs light energy at varying wavelengths, there are several of them each of different color to capture more of the available light energy.

There are three basic classes of pigments: chlorophylls, carotenoids and phycobilins.

Chlorophyll, the green pigment, absorbs light in the violet, blue and red wavelengths. Different pigments absorb light energy at different wavelengths. The absorption pattern

of the pigment is called the absorption spectrum. The absorption spectra of chlorophyll and the accessory pigments are shown below in Figure 2.1.

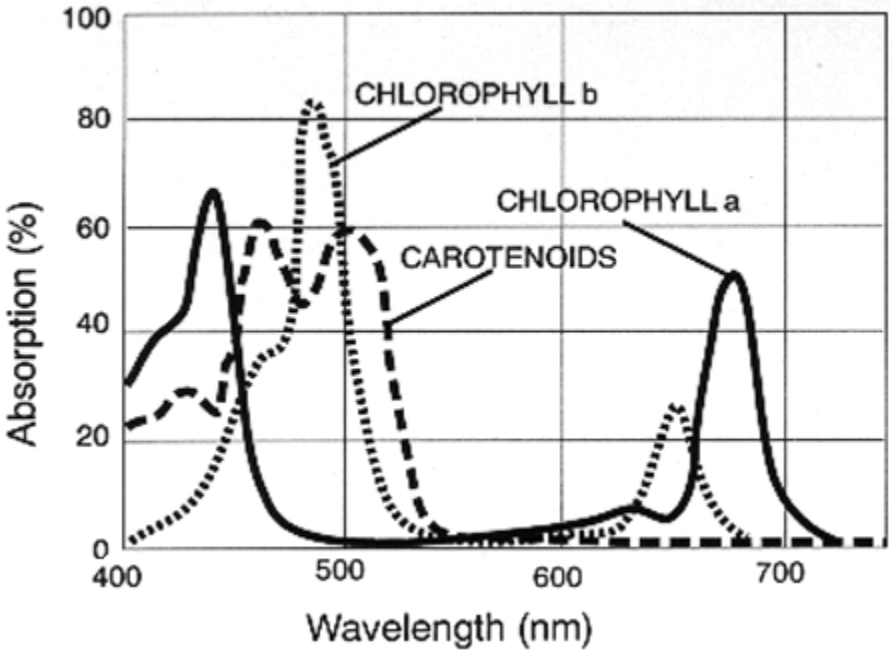

Figure 2.1.—Absorption spectra showing light absorption by chlorophyll a, b and the carotenoids. Figure from Gilmore.A.M. and Govindjee [42]

There are several types of chlorophylls; chlorophyll *a* is the major photosynthetic pigment found in all higher plants, algae and cyanobacteria. It absorbs the light energy used in the synthesis of carbohydrates from carbon dioxide and water. It absorbs its energy in blue region in the wavelengths between 422 nm and 428 nm and in the red region in the wavelengths range 660-676 nm [43] of the spectrum. Other pigments are called the accessory pigments and include chlorophyll *b, c, d*, carotenoids and phycobilins. These pigments are responsible of absorbing energy that chlorophyll *a* is unable to absorb.

Chlorophyll *b* which is present in all higher plants and green algae absorbs at different wavelengths of light other than that absorbed by chlorophyll *a*. It has its absorption maxima at 650 nm in red region and 460 nm in the blue region of the spectrum. On absorbing light, it becomes excited and transfers its energy to a chlorophyll *a* molecule.

Chlorophyll *c* (of two or more types) is present in diatoms and brown algae. It has its absorption peaks at 460 nm and 620 nm [44]. Chlorophyll *d*; isolated from red marine

algae, hasn't been shown to be present in the living cells in large enough quantities to be observed in the absorption spectrum of these algae. It has three main absorption maxima at 696nm, 455 nm and 400 nm with its main absorption band in the red region.

Caroteinoids are found in all photosynthetic organisms and also in some non-photosynthetic bacteria, yeasts and molds. They have their absorption in the range of 460 nm-540 nm wavelengths for their corresponding maxima and minima [45].

Photosynthesis is broadly described in two stages; the light dependent reactions or light reactions and the light independent reactions or the dark reactions. The light-dependent reactions consist of photochemical reactions which are carried out by two photosystems called photo system I (PS-I) and photo system II (PS-II). Each photosystem unit contains about 250 to 400 molecules of pigments which include chlorophyll molecules and accessory pigments [5] located in the thylakoid membrane. These serve as the antenna complexes. The thylakoid are stacked in grana held within the stroma of chloroplasts.

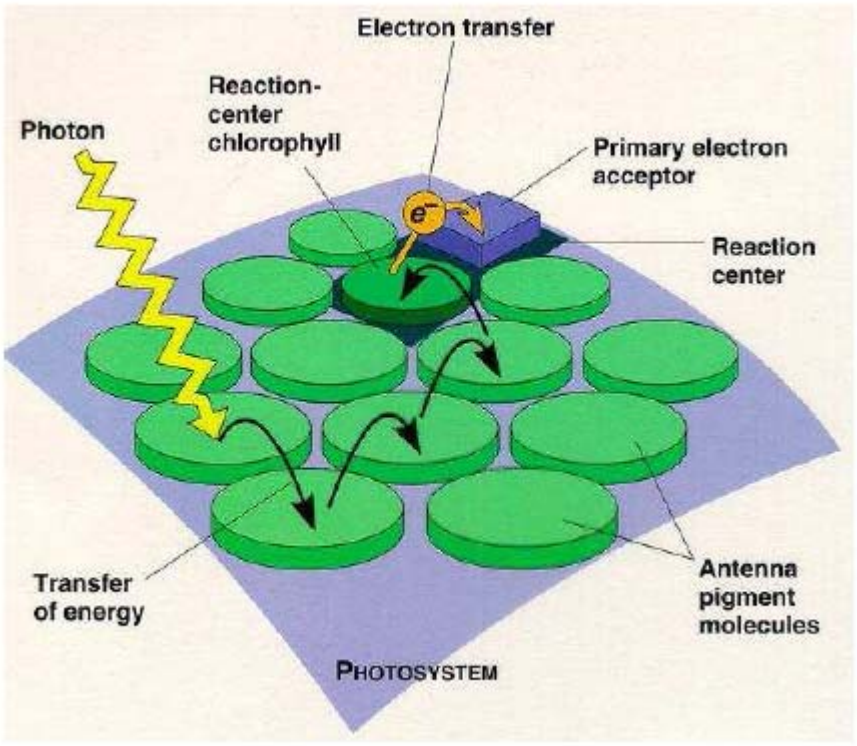

Figure 2.2: The photosystem. The light energy is absorbed by the antenna pigment molecule which transfers it to a nearest molecule until it reaches the reaction center which becomes ionized and losses its electron to an electron acceptor. Figure adapted from [46]

Photosystem-I contains chlorophyll *a* molecule known as P700 because it has an absorption peak at 700 nm. Photo system-II contains chlorophyll *a* molecule referred to as P680 because its absorption peak is has at 680 nm.

Antenna complex serves to harvest light energy and transfer the excitation energy to the complex of chlorophyll molecules and proteins called the reaction center (RC). The two photosystems are associated with reaction centers RCI and RCII respectively.

2.3 Light and dark reactions

In light reactions, energy from absorbed photon is used in the splitting of water molecules to form electrons, protons and oxygen as shown in the equation below.

$$2H_2O \rightarrow 4e^- + 4H^+ + O_2 \qquad 2.1$$

The electrons are then transferred from water (with redox potential of ~+0.82V) to nicotinamide adenine dinucleotide phosphate ($NADP^+$), the oxidized form by a scheme known as the Z- scheme shown in Figure 2.3. This leads to the production of oxygen and NADPH (with redox potential of ~-0.32V) the reduced form of NADP. The adenosine disphosphate (ADP) and the inorganic phosphate (Pi) are also converted to the energy rich compounds ATP (adenosine triphosphate).The equation of the reaction can be summarized as follows

$$2H_2O + 2NADP^+ + 3ADP + 3Pi \xrightarrow{hv=8photons} O_2 + 2NADPH + 3ATP$$

In dark reactions no light energy is needed. It uses the two compounds, NADPH and ATP from light reactions to convert carbon dioxide to carbohydrates. The ADP and NADP are made available to carry on the process. The equation for dark reactions is shown below

$$CO_2 + 3ATP + 2NADPH + 2H^+ \rightarrow \frac{1}{6}C_6H_{12}O_6 + 3ADP + 3Pi + 2NADP^+ + H_2O$$

2.4 The principles of photosynthesis

Light reaction photosynthesis starts with the absorption of light by the light-harvesting antenna (LCHII) of PSII where it raises the energy levels of the electrons. The excitation energy is then transferred to the RCII of chlorophyll *a* molecule (P680) of PSII which enters the excited state P680*. Within picoseconds of P680* formation of primary charge separation occurs, in which an electron is donated from P680* to pheophytin ($Pheo \rightarrow Pheo^-$) and a primary radical pair ($P680^+Pheo^-$) is formed. The electrons pass an electron transport chain (ETC) via several redox reactions to PSI following the Z-scheme shown below

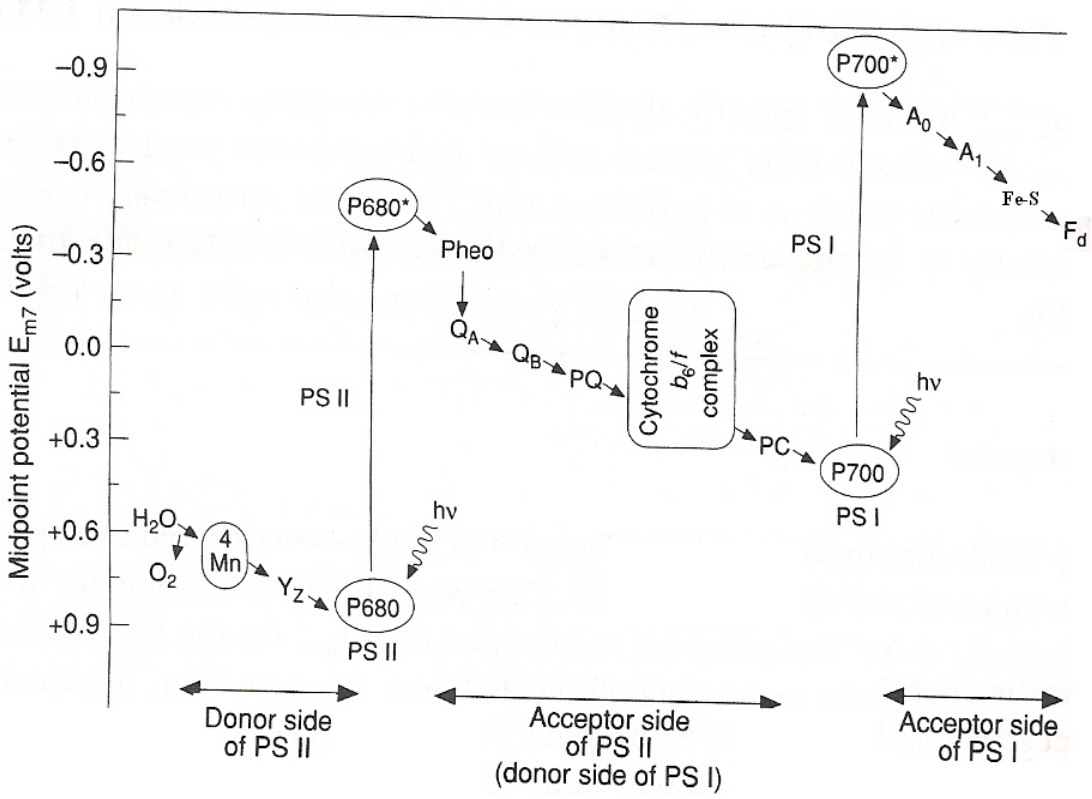

Figure 2.3: The Z-scheme showing the photosynthetic electron pathway from water (H_2O). Figure from Falkowski and Raven [47]

$P680^+$ receives an electron from tyrosine Y_Z residue which in turn is reduced by an electron from water via water splitting manganese protein complex. The manganese protein oxidizes water to produce oxygen (O_2) and protons (H^+) into the lumen.

$Pheo^-$ continues an electron transport by reducing the primary electron acceptor, a plastoquinone molecule ($QA \rightarrow QA^-$) which in turn reduces a plastoquinone molecule ($QB \rightarrow QB^-$) a secondary electron acceptor. Repeating this process QB^- accepts a second electron and removes a proton from each of the two stroma-based water molecules forming plastoquinol (PQH2O). The overall reaction taking place at PSII is given below

$$2H_2O + 2PQ \xrightarrow{hv} O_2 + 2PQH_2 \qquad 2.3$$

PQ and PQH_2 are oxidized and reduced plastoquinone molecules

The reduced plastoquinone molecule (PQ) diffuses randomly in the thylakoid membrane to the cytochrome bf complex. The cytochrome bf complex removes the electrons from the reduced PQ and facilitates the release of the protons ($2H^+$) into the inner thylakoid space. The cytochrome bf complex delivers electrons to P700 (PSI) by diffusion through the thylakoid lumen via a small copper protein, plastocyanin (PC).

In PSI light is absorbed by antenna pigments in a light-harvesting complex (LHCI) and the excitation energy is transferred to the primary electron donor of PSI (P700) that causes further charge separation between P700 and the primary acceptor Ao (a chlorophyll monomer). The $P700^+$ formed is in turn reduced by plastocyanin. The electron on Ao is transferred to a number of iron-sulfur (Fe-S) proteins via phylloquinone molecule (A1). The Fe-S protein reduces the water soluble protein called the ferredoxin (Fd) and this occurs in the stromal side of the thylakoid membrane. The reduced equivalents from the reduced ferredoxin are used to reduce $NADPH^+$ to NADPH, which reaction is catalyzed by the enzyme Fd-NADPH reductase. The overall flow of electrons in the Z-scheme (Figure 2.2.) is summarized below

$$H_2O \rightarrow PSII \rightarrow PQ \rightarrow Cyt.b_6f \rightarrow PC \rightarrow PSI \rightarrow Fd \rightarrow NADP^+$$

The electrochemical proton gradient generated during the light reactions is used by ATP synthesis from ADP and Pi. The linear electron flow of the Z-scheme may become disrupted when PSI cannot receive an electron from PSII. In this case the oxidation of plastoquinone is the slowest reaction in the electron transfer [48]. It therefore becomes possible for cytochrome bf to be oxidized whilst PQ remains reduced. This leads to electrons to start cycling around PS-I, passed from ferredoxin back to cytochrome bf complex. In this cyclic electron transfer the energy is used only in the generation of a proton motive force and ATP formation but not NADPH.

The next step of photosynthesis is the consumption of NADPH and ATP for assimilation of carbon dioxide, resulting in the formation of carbohydrates.

2.5 Photosynthetic oxygen formation

Photosynthetic oxygen evolution results from water oxidation during the light phase of photosynthesis in plants and algae. The process of the oxidation of water to produce oxygen is done by the oxygen evolving complex (OEC). The OEC at the PSII donor side (where light reaction takes place) comprise a redox-active tyrosine Yz and a tetra nuclear manganese cluster that binds two substrate water molecules and accumulates oxidizing equivalents [49]. The S-state cycle identifies the number of oxidizing equivalents stored and oxygen is released on the transition from S_3 to S_4 to S_0. These oxidizing equivalents are generated when photon energy is absorbed and transferred to a primary electron donor, P680.

Driven by the sequential absorption of four light quanta, the OEC is stepped through its reaction cycle [50]. Upon excitation of P680 after the absorption of a photon, a chlorophyll cation ($P680^+$) is formed and this oxidizes Yz.

$$Yz\ P680^+ \rightarrow Yz^{\bullet} P680 + H^+ \qquad 2.5$$

The tyrosine radical $Yz^{\bullet}$ then extracts the electron from the manganese cluster.

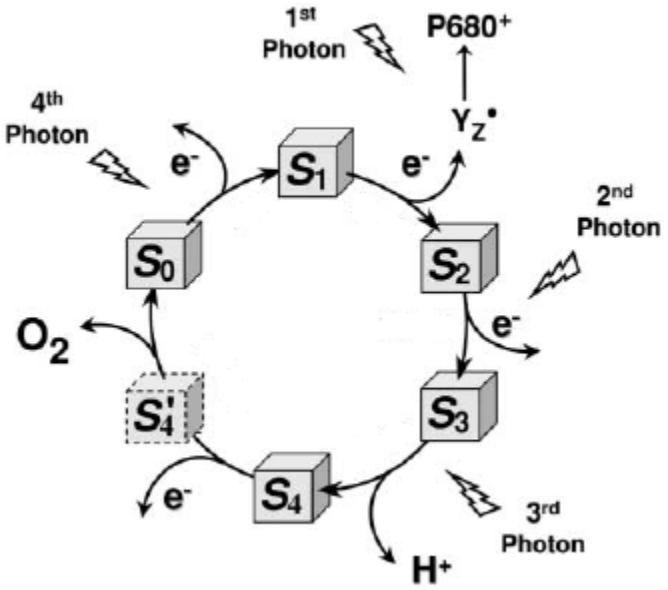

Figure 2.4: Extension of the classic S-state cycle of the photosynthetic oxygen evolving complex in the reaction center of PSII. Figure from Haumann et al [50]

In the most reduced state S_0, two molecules of water are bind to the complex. The S_1 state is dark-stable, S_2 and S_3 are formed by one and two light driven oxidation steps, respectively. The third photon induces $S_2 \rightarrow S_0$ states transition. At each step of the cycle an electron and proton are removed, causing one of the Mn ions to achieve higher oxidation state. These electrons are transferred, one at a time via a tryrosine residue Yz to the oxidation reaction center of PSII. After the most oxidized S_4 state is generated, oxygen is released, lowering the oxidation state of Mn complex by two positive charges and regenerating the starting S_0.

2.5 Effects of UVR on photosynthesis

UVR reduce photosynthetic rates of micro-algae by direct effects on the photosynthetic apparatus as well as via indirect effects, such as DNA damage.

2.6.1 Direct effects

The adverse effects of UVR exposure on photosynthesis result from the absorption of high energy-radiation by biomolecules such as proteins. The D1 protein in the core complex of photosystem II and the carbon dioxide –fixing enzyme RubsiCO have been identified as the major targets of UV exposure [51] [52].

PS-II sensitivity to UVR is explained by UV active chromosphores present on both acceptor and donor sides PSII. On the acceptor side UVR targets of PS-II include the plastoquinones and D1 protein itself [53] [54]. On donor side Y_Z and the oxygen evolving manganese (Mn) cluster are the possible UV active chromosphores (see Fig 2.2).

Damage on the acceptor side of PS-II [55] [56] have been detected when PS-II preparations or thylakoid are exposed to high energy-radiation. This results in the complete reduction of plastoquinone pool, leaving the QB^- site nonoperational because of lack of reducible plastoquinone molecules [57]. Because the singly reduced primary quinone acceptor (QA^-) cannot transfer its electron to QB, QA^- becomes doubly reduced to (QA^{2-}). It is then protonated and forms QAH_2, which is released from its binding site on the D1 protein [58]. With this empty site, chlorophyll (P680) excitation results in the formation of a primary pair, $P680^+$-$Pheophytin^-$. The recombination of these radicals allows the formation of chlorophyll triplets that react with oxygen to form singlet oxygen, which ultimately damage the D1 protein.

PS-II photoinactive (photoinhibition) also occurs when the donor side of it is unable to keep up with the rate of withdrawal of electrons from P680 [59]. This photoinhibition may be triggered by absorption of light by the manganese cluster of the oxygen evolving complex of PSII. Excitation of manganese cluster leads to a reversible inactivation of the OEC. When OEC is inactivated, photoinhibition would proceed due to the formation and accumulation of long-lived highly oxidizing radicals, such as Y_Z and $P680^+$. Those oxidizing species can rapidly inactivate the electron transport, damage proteins and inhibit the *de novo* D1 protein synthesis.

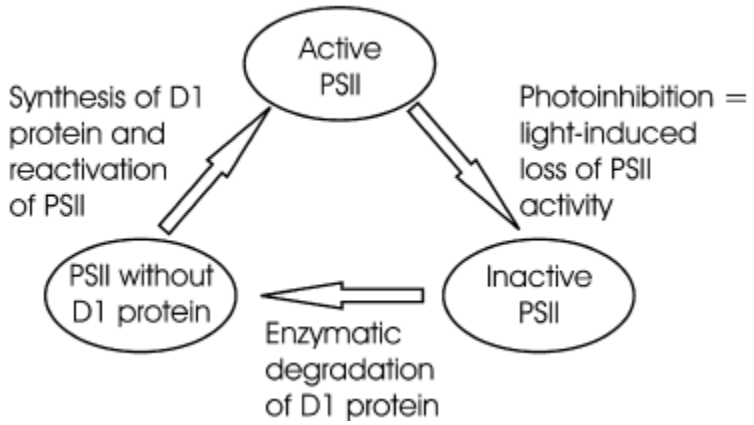

Figure 2.4: Schematic representation of photoinhibition and repair of photoinhibited PSII. Figure from Tyystjärvi [60]

2.6.2 Indirect effects

All organisms that are regularly or occasionally exposed to UVR may be subjected to DNA damage. DNA is one of the most UV-B sensitive molecules. UV-B can cause dimerization of DNA bases, leading to the formation of photoproducts such as cyclobutane dimmers [61]. These photoproducts block DNA transcription and replication such that only a single distortion of DNA may be sufficient to stop DNA replication. They may hinder cell cycle progress and replication because they obstruct *de novo* synthesis of cellular components and substances required for growth and cell maintenance. As a consequence, a number of physiological processes such as photosynthesis [62] are affected.

2.6 Mechanism to reduce the effects of UVR on photosynthesis

Adaptation to UVR assumes the existence of mechanisms that protect organisms or reduce the deleterious effects. However the protection of micro-and macro algae against UVR may result into reduced growth and primary production [63]. There are four basic mechanisms that can be adapted by the organisms to cope with the UVR exposure [64].
Avoidance mechanism is a common strategy against exposure to high levels of UVR. For microalgae such as diatoms possess the ability of downward migration into the substrata

to reduce on UV exposure. Avoidance can also be achieved by means of circadian rhythms that allow an organism such as microalgae to swim down to depth where radiation intensities are low, as occur in some dinoflagellates [65].

Another strategy to minimize the effects of UVR is through the presence of UV-screening compounds such as mycosporine-like amino acids (MAAs). MAAs are water soluble compounds with an absorption maxima between 310 and 360 nm which are found in many marine and fresh water microalgae and heterotrophic organisms [66]. Typically absorbing in the UVA and UVB range, these biomolecules were invoked to function as passive shielding solutes by dissipating the absorbed short wavelength radiation energy in form of harmless heat without generating photochemical reactions [67]. These compounds have been proved to be an effective protection mechanism [68] so that photosynthesis in phytoplanktonic cells with higher amounts of MAAs was less inhibited. In some diatoms, however, the production of such protective substances does not appear to be a major strategy. Other compounds such as scytonemin a UV-absorbing extracellular substance, phlorotanins found in brown algae and coumarins found in green algae may also have a protective role, functioning as UV-screening agents [69]. In addition, high concentrations of carotenoids as a result of UVR exposure have been observed in diatom mats [70], suggesting an UV-protecting function of these pigments.

In addition, and while UVR –mediated DNA damage occurs in aquatic autotrophic organisms such as microalgae [71] repair mechanisms of DNA molecule [72] are also present [73]. However, the presence of one or other mechanism (i.e. photoreaction, nucleotide excision repair or recombination pair) is clearly dependent on the species under study and radiation conditions at which the cells are exposed [72].

Finally, acclimation mechanisms to cope with high UVR intensities are important in several microalgae. These usually occur on a long-term basis, when microalgae have been exposed for enough time to UVR. One of these acclimation mechanisms is the already mentioned synthesis of MAAs as found in some cultures of phytoplankton. Acclimation can also occur through a change in the community composition [74], so that

these species more adapted to a particular light regime will dominate. Therefore the responses are strongly specie-specific and depend on radiation levels and the quality to which the organism are exposed.

3 The principle of the 10-channel Fiber-Optic Oxygen Meter (oxy-10)

3.1 The oxy-10 meter

The OXY-10 micro meter is an oxygen meter, which uses the fiber optical oxygen micro sensor. The OXY-10 system detects oxygen in both liquids and the gas phase. It consists of 10 independent channels for simultaneous or sequential measurements.

Figure 3.1: The oxy-10 micro meter

The oxy-10 meter can measure oxygen in percentage air saturation (%as), Torr, hpa, mg/l or mmol and is controlled by using software which saves and visualizes the measured values. It does not contain temperature sensors and temperature changes during the measurements are not compensated by its software

3.1.1 The fiber optical micro sensor

Micro sensors with dimension of <50 µm are ideal tools for determining oxygen gradients at high spatial resolution and oxygen production and consumption [75] They are suited for sensing even very low levels of dissolved oxygen which are typical in marine and fresh water.

The limit of detection of the oxygen micro sensors is 0.15 % air-saturation which corresponds to 15 ppb dissolved oxygen and it has a measuring range from 0-50 % oxygen saturation (0-250 % air saturation).

The fiber optical sensor consists of a polymer optical fiber with a polished tip which is coated with a planar oxygen–sensitive foil in which chemical reactions and luminescence reaction takes place [76]. The end of the polymer optical fiber is covered with a high-grade steel tube to protect both the sensor material and the fiber. Usually the fiber is coated with an optical isolation sensor material in order to exclude ambient light from the tip and improve on chemical resistance which slows down the sensor response. This optical isolation layer also prevents any chlorophyll excitation if a plankton sample is measured, which may otherwise lead to wrong oxygen values. The response time of the optical isolated oxygen sensor in a stirred solution is <30 s and <60 s in a non-stirred solution and <10s in the gas phase.

Figure 3.2 shows a set up of a fiber optical micro sensor (micro optode).

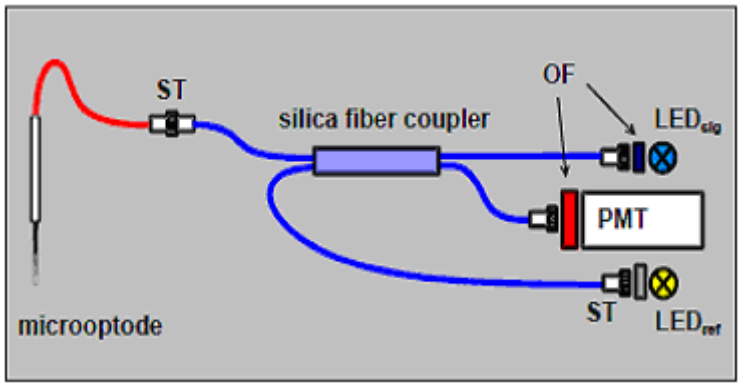

Figure 3.2: A set up of the fiber optical micro sensor [77]

The set up consists of a bright blue light emitting diode (LED) as a light source with a maximum emission at 470 nm, a multimode fiber coupler to split the beam, a reference photodiode and a compact red-sensitive photomultiplier tube module (PMT) equipped with a an optical filter (OF) (a band pass filter) with transmission within a range 510-570 nm. The LED intensity is directly modulated and light power controlled at a frequency of 750Hz by an integrated circuit [78].

3.2 Spectroscopic principles of optical sensing

The microoptodes that use dye materials apply basics of spectroscopic principles. When light energy interacts with the outer electrons of the dye molecules, the atomic structure and other optical properties of the dye are changed by chemical reaction or a change in the molecular environment. This can be due to protonation, oxidation or the presence of special kind of species.

The energy of the incident light is absorbed by the dye, which occurs only when the energy levels within the molecular system corresponds to the incident energy levels.

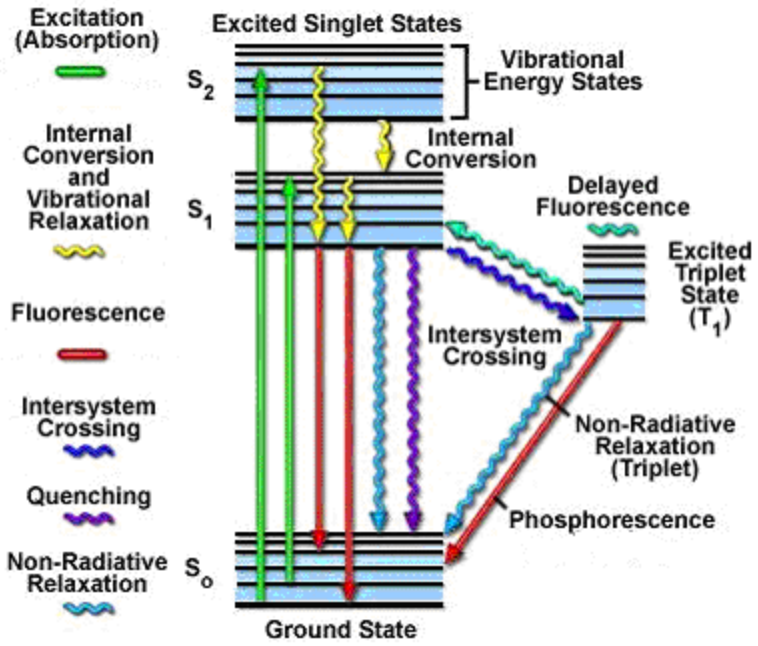

Figure 3.3 Jablonski diagram showing energy level schemes with the energetic ground level S_O, the excited singlet levels S_1 and S_2, and an excited triplet level T_1.

As shows in Figure 3.3, the dye molecule is raised from the ground state S_O to excited levels S_1 and S_2 respectively depending on the light energy. The electron spin in the singlet excited state is opposite to that in S_O. Therefore the transition from the singlet excited state to the ground state doesn't require spin adjustment.

The excited electronic state consists of vibrational energy levels with much small energy spacing (S_1 and S_2).

Once in the excited singlet state, some dyes may exhibit relaxation to S_O via repetitive energy transfer to rotational and vibrational levels and on Figure 3.3 this is shown between S_1 and S_2 and these are referred to as the absorption dyes. The fiber optical sensors with the dye immobilized at the fiber tip measure absorption, via the reflected and back scatted light from the fiber tip.

Other dyes may return to S_O by emission of a photon with less energy than the absorbed due to vibrational relaxation prior to photon emission. The emission spectra of these dyes are shifted towards the red part of the spectrum as compared to the excitation spectrum

and this effect is called Stokes shift. The transition from S_1 to S_O leads to emission of light as fluorescence. Conversion from the S_1 to triplet exited state (T_1) is a slow process known as intersystem crossing that accompanies the fluorescence–generating transition between singlet states. The electron spin in the in T_1 is parallel to that in the singlet ground state. Therefore, a transition from T_1 to S_O is forbidden. Such emission is known as phosphorescent. This occurs only when there is a strong interaction in the dye molecules. These two processes, fluorescence and phosphorescence are referred to as photo luminescence. This is applied in luminescence dyes which enable measurements at wavelengths different from the absorption allowing efficient separation from the background signal. Molecules like oxygen are able to absorb energy from the excited dye by collision. The dye returns to the ground state without emitting a photon. The luminescence is quenched as a function of the amount of quenching molecules present which changes the intensity of the emitted radiation and the lifetime of the luminescence. This principle is used in the measurement of oxygen concentration.

3.2.1 **Principle of the fiber optical micro sensor**

The principle of the fiber optical oxygen micro sensor is based on the dynamic luminescence quenching [79] by the molecular oxygen. When the modulated light with peak wavelength 450nm [75] from the blue LED is incident on the florescent dye molecule (luminophore) it excites the dye molecule. The molecule returns to its ground (triplet) state by emitting fluorescence light of long wavelength (see Figure.3.4 (1)) of a maximum wavelength of 610nm [80] that travels back and is detected by a red-sensitive photomultiplier tube module or photodiode with a band pass transimpedance amplifier that is adapted to the light modulation frequency (750Hz) and signal form.

The DC offset of the photodiode is cut off by a high-pass filter $f_c = 8\text{K Hz}$ [81]. The measuring signal is rectified, sent through a low pass filter f_c=20 KHz [82], and amplified in order to minimize the influence of ambient light or electronic noise. This DC voltage signal is displayed on a voltmeter display and is available via a computer.

When the light-emitting fiber tip is moved towards the water/sample interface containing the dissolved oxygen, it illuminates the sample around the tip and excites the

fluorescence dyes present. The oxygen molecules in the sample diffuse into the sensor tip and collide with the excited fluorescent dye molecules. Then collision between the fluorescent dye molecule (luminophore) in its excited state and the oxygen (quencher) results in radiation less deactivation and is called collisional or dynamic quenching shown in Figure.3.4 (2). After the collision, energy is transferred from the excited fluorescent dye molecule to oxygen which consequently is transferred from its ground state (triplet state) to its excited singlet state. As a result the fluorescent dye molecule doesn't emit light intensity and the measurable intensity signal as well as the lifetime of the excited state of the fluorescent dye molecule decreases.

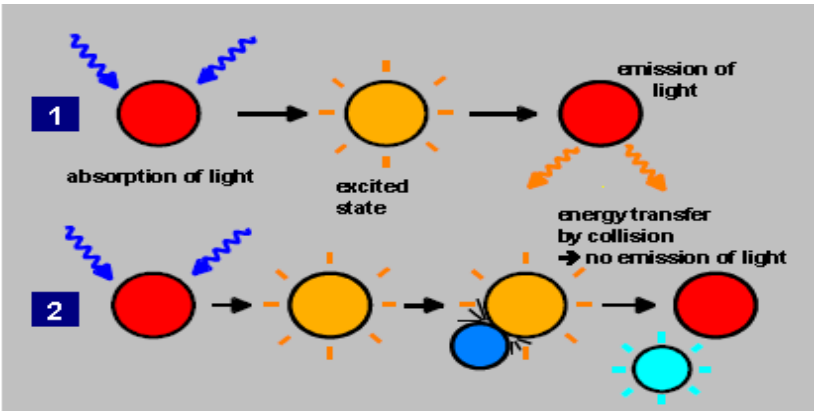

Figure 3.4: Principle of dynamic quenching of luminescence by molecular oxygen. (1) Luminescence in absence of oxygen. (2) Deactivation of the luminescent indicator molecules by molecular oxygen. Figure from [77]

The relation between the oxygen concentration and the luminescence intensity as well as the lifetime of the excited state of the luminophore is described by the Stern-Volmer equations:

$$\frac{I_O}{I} = 1 + K_{SV}[O_2] \qquad 3.1$$

$$\frac{\tau_O}{\tau} = 1 + K_{SV}[O_2] \qquad 3.2$$

I and I_O are the luminescence intensities in presence and absence of oxygen, τ and τ_O are the luminescence excited state lifetimes in presence and absence of oxygen, K_{SV} is

the overall quenching constant (Stern-Volmer constant), and $[O_2]$ the oxygen content. The Stern-Volmer constant quantifies the quenching efficiency and therefore the sensitivity of the sensor.

However equations 3.1 and 3.2 are only valid if the luminophore is located in a homogeneous environment, and displays a linear correlation between I_O/I or τ_O/τ and the oxygen concentration $[O_2]$.

Oxygen sensors based on measurements of light intensity have some draw backs. These include susceptibility to light source and detector drift, to changes in optical path and drift due to degradation of leaching of the dye [80]. Also other practical problems associated with the sensors have been observed [82] which include bending effects and consequent change in the signal intensity. If the sensing tip penetrates a rigid or a very cohesive material, the micro bending of the fiber tip may affect the oxygen measurements.

There is also a problem of decrease in the signal intensity [81]. This is caused by a black isolating coating that excludes optical interferences from the heterogeneous sample which may be caused by for example scattering effects; chlorophyll fluorescence etc. These disadvantages can be reduced by operating a sensor based on luminescence lifetime instead of luminescence intensity. This is because lifetime, τ, is an intrinsic property of the fluorescent dye which is independent of external perturbation unlike intensity. The life time is quenched in the presence of oxygen described in equation 3.2. Lack of optical isolation can however; cause another problem. This can be observed in phototrophic communities where the excitation light can stimulate photosynthesis at the sensing tip. This can cause an increase in oxygen values. This problem can also be solved by using a new oxygen indicator excitable with NIR LEDS or a proper time regime to reduce photosynthesis effects [81].

4 MATERIAL AND METHODS

4.1 LABORATORY EXPERIMENTS.

4.1.1 An experimental system (Photoinhibitron) for testing the effects of UVR on phytoplankton

A photoinhibitron is a special incubator used to investigate the inhibition of the phytoplankton photosynthesis by UVR.

The effects of UVR on individual organisms and physiological processes in aquatic environment have been obtained from laboratory experiments in which a high degree of control can be achieved though complex ecological interactions are difficult.

In our laboratory approach to determine the effects of UVR upon phytoplankton photosynthesis, we have designed and implemented an experimental system (photoinhibitron) which was used essentially as described below. The phoinhibitron consisted of the aluminum frame which supported an array of 17 florescent tubes of 59cm length which illuminated a temperature controlled water bath with 15 positions for sample bottles each with a diameter of 6 cm. The array consisted of 5 Philips TL20W/12 UV-B florescent lamps (Cleo professional lamps) which emitted light mainly in the range (280 to 320 nm), with a maximum range at 312 nm. UV-A was provided by 6 Philips TL20W/05 (Cleo professional) emitting light mainly in the range 320 to 400 nm with a maximum at 365 nm and 6 TLD18W/965 PAR florescent lamps emitting light in the visible range (400 to 700 nm). The order of arrangement of the tubes is shown in Figure 4. below.

Figure 4.1: The arrangement of the florescent lamps in the photoinhibitron. P-represents PAR, A-UVA and B-UVB.

UV-A and PAR irradiances emitted by the lamps under our laboratory conditions were substantially lower than a typical midsummer outdoor conditions (measured for on 26.06.2009 for comparison). However the UV-B lamps at maximum intensity emitted higher proportion of the more damaging shorter wavelength photons than would be experienced under natural conditions. The use of higher UVR was certainly to avoid the masking of PAR on UV effects and also to quickly observe these effects.

The tubes were suspended a distance of 0.2 m from the top of filters to provide homogeneous and mixed field (UVR and PAR) down-welling exposure. In addition, an intensity attenuator was also used to independently vary the UV-A, UV-B and PAR intensities. The number of lamps used in the operation and varying the distance between the florescence tubes and the water bath also enabled us to achieve a homogeneous intensity distribution. The spectral irradiances of the tubes from 280 to 700 nm were

measured by means of a RAMSES spectroradiometer and a NILU-UV irradiance meter. The spectral distributions applied by the photoinhibitron are shown in Figure 4.1 below.

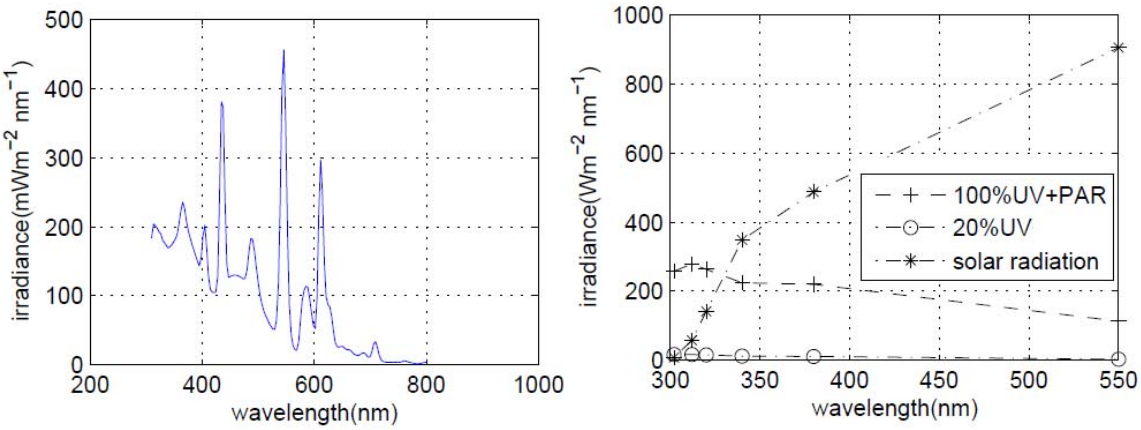

Fig.4.2: Left: Irradiance spectra of the tubes measured with RAMSES spectroradiometer. Right: Irradiance spectra of the tubes corresponding to 100% UV-A (320-400 nm), 100% UV-B (280-320 nm), 100% PAR and 20% UVR+PAR and solar radiation conditions measured with NILU-UV irradiance meter.

.

A set of 3mm thick glass sheet filters of size 5x5 cm with a normal cut off of 50%, were used to cut off different wavelength ranges from the spectrum emitted by florescent lamps.

These filters controlled the ambient light in regime in three different ways; (a) P=PAR - treatment (>400nm), using filters with cut off wavelengths 385, and 550 nm, radiations <385 and <550 nm were blocked; (b) PA=PAR+UV-A treatment (>320nm), using a filter of 320 nm cut off wavelength, radiation <320 nm was blocked, (c) PAB=PAR+UV-A+UV-B treatment (>280 nm) using a 280 nm cut off filter almost all PAR and UV radiations were transmitted.

The respective transmission spectra of these filters are shown in Figure 4.3.

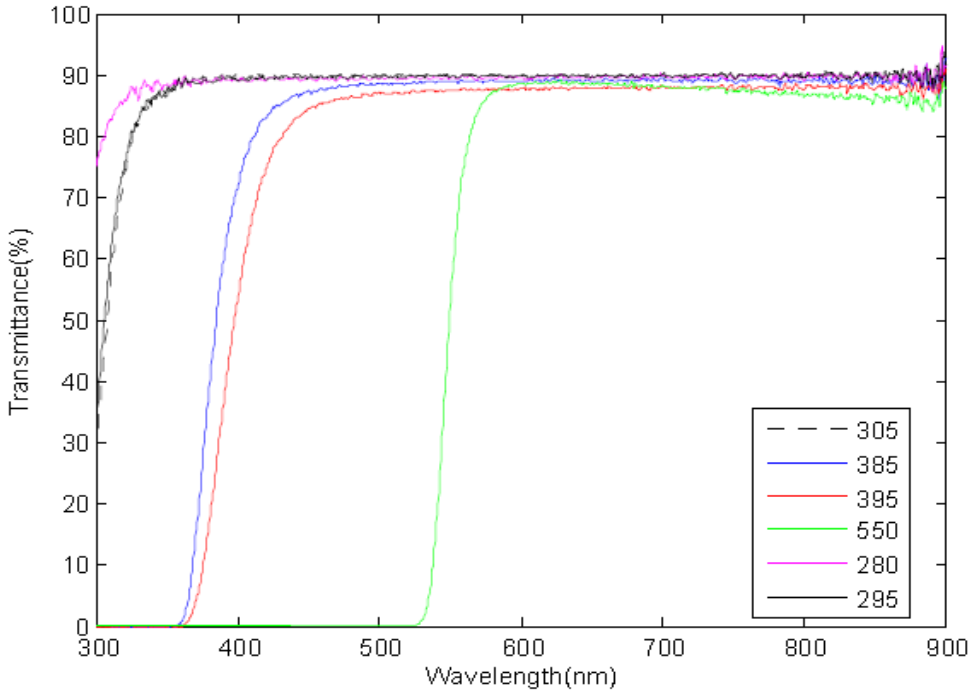

Figure 4.3: Spectral transmission characteristics for the log pass cut off filters used as measured by the UV-VIS recording spectrophotometer.

The photoinhibitron was built in such a way that all experiments on algae were conducted at the respective temperatures at which the algae were grown.

Figure 4.4: The complete set up of the photoinhibitron used to expose algae to different wavelength of light.

Figure 4.5: The set up of the water bath with the sample bottles in the photoinhibitron.

Because of the strong thermal radiation emitted from the light source, cooling water was pumped through the water bath in order to keep the temperature constant throughout the incubation. The cooling water was recycled through a plastic tank and a digital thermostat was used to control a water cooler in order to keep this water at a constant temperature. The temperature of water in the tank was measured throughout the experiment. The lamps were turned on for atleast 20 minutes (Figure 4.5) prior to the incubation to stabilize the light intensity.

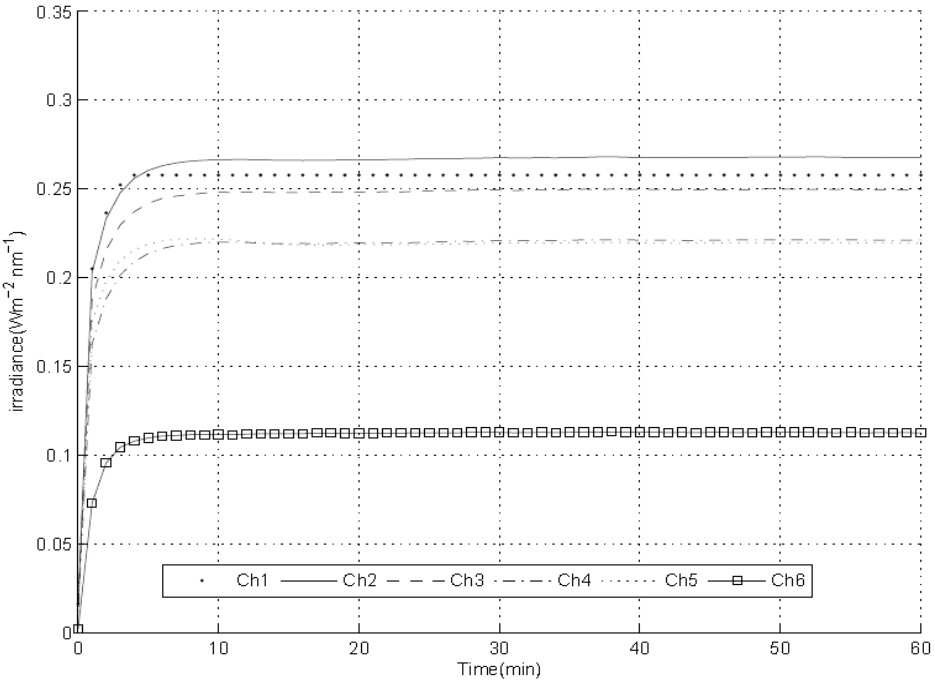

Figure 4.6: The variation of irradiances with time as measure by the six channel (Ch) NILU-UV irradiance meter with center wavelengths at 302 (Ch1), 312 (Ch2), 320 (Ch3), 340 (Ch4), 380 (Ch5) and 550 (Ch6).

4.1.2 Irradiance measurements

The irradiance levels during the laboratory experiment were measured. The irradiance on which algae was growth, was measured using a scalar 4Л irradiance sensor (Biospherical Instrument QSL-100, San Diego, USA). The irradiance during the incubation was measured using NILU-UV irradiance meter. It is a multi channel radiometer which

measures UV irradiances at five channels with center wavelength at 302, 312, 320, 340 and 380 nm. The channel bandwidths are approximately 10 nm at full width half maximum (FWHM). In addition, a sixth channel measures photosynthetic active radiation (PAR) in wavelength region $400<\lambda<700$ nm with center wavelength at 550 nm.

4.1.3 Cultures

Cultures were grown in glass culture tubes at the Department of Microbiology University of Bergen. The tubes were placed in the water bath, and the temperature of the water bath was kept between 18 and 20^{o} to ensure that it was constant and was monitored using thermostats. The water bath was then illuminated by two florescent lamps (Philips TLD 58W/830). The illumination was continuous providing irradiance (PAR) of $27Wm^{-2}$. The algae were grown in fresh and marine water nutrient media. Each week new experimental cultures were grown to minimize risks of contaminations. Carbon dioxide enriched humified filtered air was bubbled through cultures inside the culture tubes. This was to ensure that the growth was not limited of carbon dioxide one of the requirements for photosynthesis to take place. In addition, bubbling distributed the algae cells homogenously throughout the culture tubes. The growth rate of the cultures were maintained semi-constant and cell densities maintained in the order of 10^6 to 10^7 cells ml^{-1} by diluting the cultures every two days. Before each set of measurements, the samples to be tested were isolated from the culture in the culture tubes. Their concentration or density was measured using a microscope. Sub samples from the culture tubes were transferred to a 120ml bottles after being diluted to a concentration of $2.2x10^5$ cells ml^{-1} with the nutrient media containing the best composition for the cell growth.

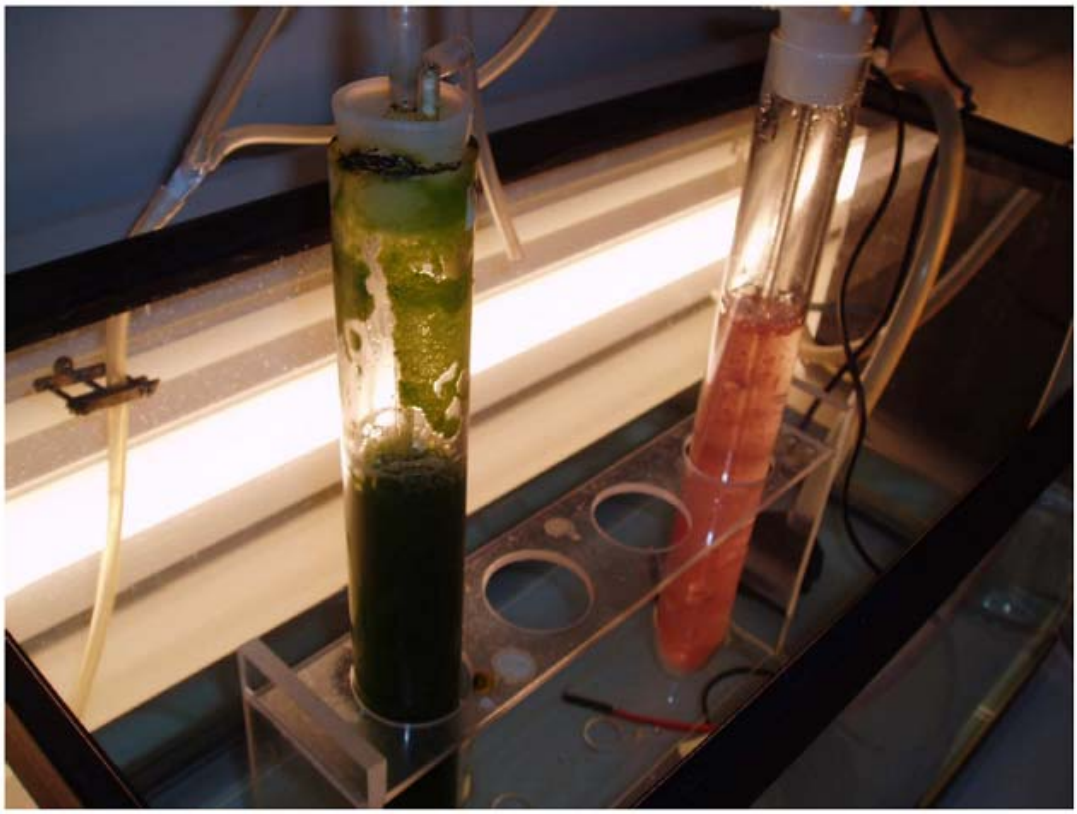

Figure 4.7: The set up showing glass tubes where algae cultures were grown.

4.1.4 Measurements of photosynthesis (oxygen measurements)

Oxygen evolution was measured in temperature controlled water bath as described in section 4.1.1. The temperature controlled water bath was used because temperature induced changes in the system interferes any photosynthetic rate measurement of the environmental samples. A temperature sensor was used to monitor any temperature changes at the on and off switches of the thermostat's heating unit. Prior to incubations, samples were filled completely in 120 ml bottles, and were sealed using lids such that there was no head space for air. In addition this also helped to avoid potential pressure to accumulate from the photosynthetic oxygen production. The bottles containing the samples (120ml bottles) were placed in the water bath controlled in the temperature range 18-20^{o} by circulating water flow and were then illuminated by the light tubes as already described in section 4.1.1.

Gentle mixing of the samples was done with magnetic stirrers in each bottle. This was done to prevent oxygen gradients inside each bottle.

Oxygen concentrations in the experiment were measured with DP-PST3 oxygen sensors (PreSens GmbH, Germany). The principle of operation of these types of oxygen sensors was described in Chapter 3 section 3.2.1. This process guarantees a high temporal resolution and a measurement without drift, oxygen consumption, or gas exchange between the incubation chamber and the environment [76]. The oxygen sensors were connected to the 10 channel-fiber optic oxygen meter fixed to the outside of the photoinhibitron. The sensors were inserted as low as possible into the 120ml bottles, placing the sensor tips through holes made in the bottles approximately 3cm below their edge. The data from the oxygen sensors connected to the oxygen meter was acquired every 15 seconds and recorded on a laptop computer. Oxygen evolution in mg O_2 L^{-1} was plotted as a function of time. The data from a certain observed interval were adjusted to a linear (best fit) so that the slope represented the oxygen production rates in mg O_2 $L^{-1}min^{-1}$.

The relative inhibition due to UVR was calculated as follows

$$P_{Inh} = \frac{P_{PAR} - P_{tot}}{P_{PAR}} \qquad (4).$$

Where P_{PAR} represents the amount of oxygen in PAR only-treatment and P_{tot} represents the amount of oxygen in any of the PAR+UVR treatments.

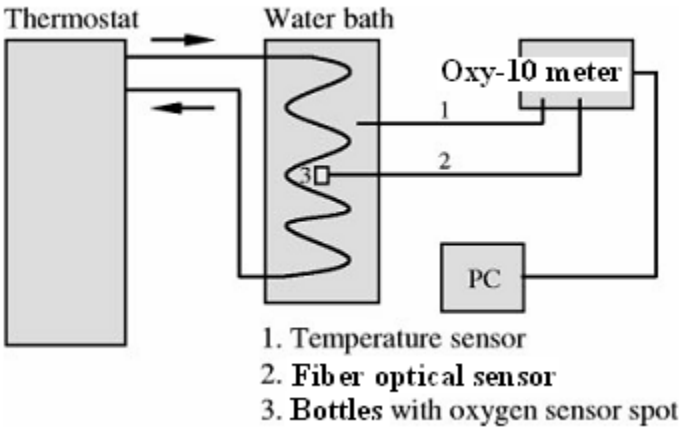

Figure 4.8 The technical setup of oxygen measurement method. Figure adopted from Warkentine et al [76].

4.1.5 Calibration of the fiber optical micro sensors

The calibration of the oxygen sensors was performed using a conventional two-point calibration in oxygen –free water (cal 0) and water vapor saturated air or air-saturated water (cal 100). In preparation of calibration standard (cal 0), 1g of sodium sulfite (Na_2SO_3) was added to a vessel. It was then dissolved in 100ml water by shaking for approximately one minute when the vessel was closed. This makes water to become oxygen free due to chemical reaction of oxygen with Na_2SO_3.

To prepare the calibration standard cal 100 (air-saturated water), 100ml of water were added to a vessel. Air was blown into water using an air-pump with a glass-frit, creating a multitude of small air bubbles, while stirring the solution to obtain air-saturated water. After 20 min the air-pump was switched off and the solution was further stirred for 10 min to ensure that water was not super saturated.

After preparing the calibration standards, performing of the calibration started by switching on the oxy-10 and the PC software. In the software there is calibration window where the actual atmospheric pressure (in hpa) and the temperature of calibration standards cal 0 and cal 100 are entered. The atmospheric pressure of the calibration is needed to convert the oxygen unit % air-saturation into partial pressure units (hpa, Torr) or connection units (mg/L, μmol/L). The channels to be calibrated were then selected in the section channel of the sub window SINGLE CHANNEL or ALL CHANNELS.

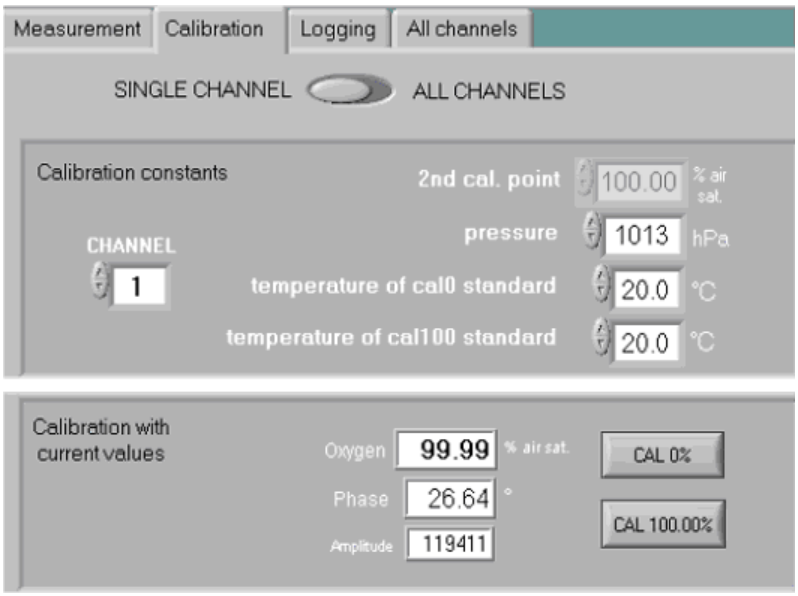

Figure 4.9: showing the calibration window [77].

Using the oxygen sensors calibration was performed at constant phase angles and the calibration values were stored at adjusted temperatures.

5 Results and discussions

In February 2009, a number of marine and fresh water algae were grown, and at the same time the construction of a photoinhibitron for testing the effects of UVR and PAR on photosynthesis started. Since then several experiments have been done to test how photosynthesis varies with different PAR irradiances and the effects of PAR+UVA and different levels of UVB on photosynthesis have been investigated. The table below shows the different types of algae species that have been grown and tested in our experimental system.

Species	**Algae type**
Amphidinium carterae	Dinoflagellate
Emiliania huxleyi	Coccolithophoride
Pseudo-nitzschia calliantha	Diatom
Protoceratium reticulatum	Dinoflagellate
Proboscia alata	Diatom
Haematococcus pluvialis	Green algae
Phaeodactylum tricornutum	Diatom

Table 5.1: Overview of the different types of algae that have been grown and tested in the laboratory.

5.1 Variation of photosynthetic rate with irradiance

Under optimal conditions of carbon dioxide concentrations and temperatures, the rate of photosynthesis depends on light intensity absorbed by photosynthetic cells of the algae.
In this experiment light intensity was modified by placing the source of light (slide projector) at different distances from the experimental system. The photosynthetic rate was obtained from the rate of oxygen evolution as described in Chapter 4 section 4.1.4. Net oxygen evolution was determined from light dependence of evolution using the fiber optical micro sensor technique.

The relationship between irradiance (E) and photosynthetic rate (P) is usually represented on photosynthesis versus irradiance curve as shown in Figure 5.1.below.

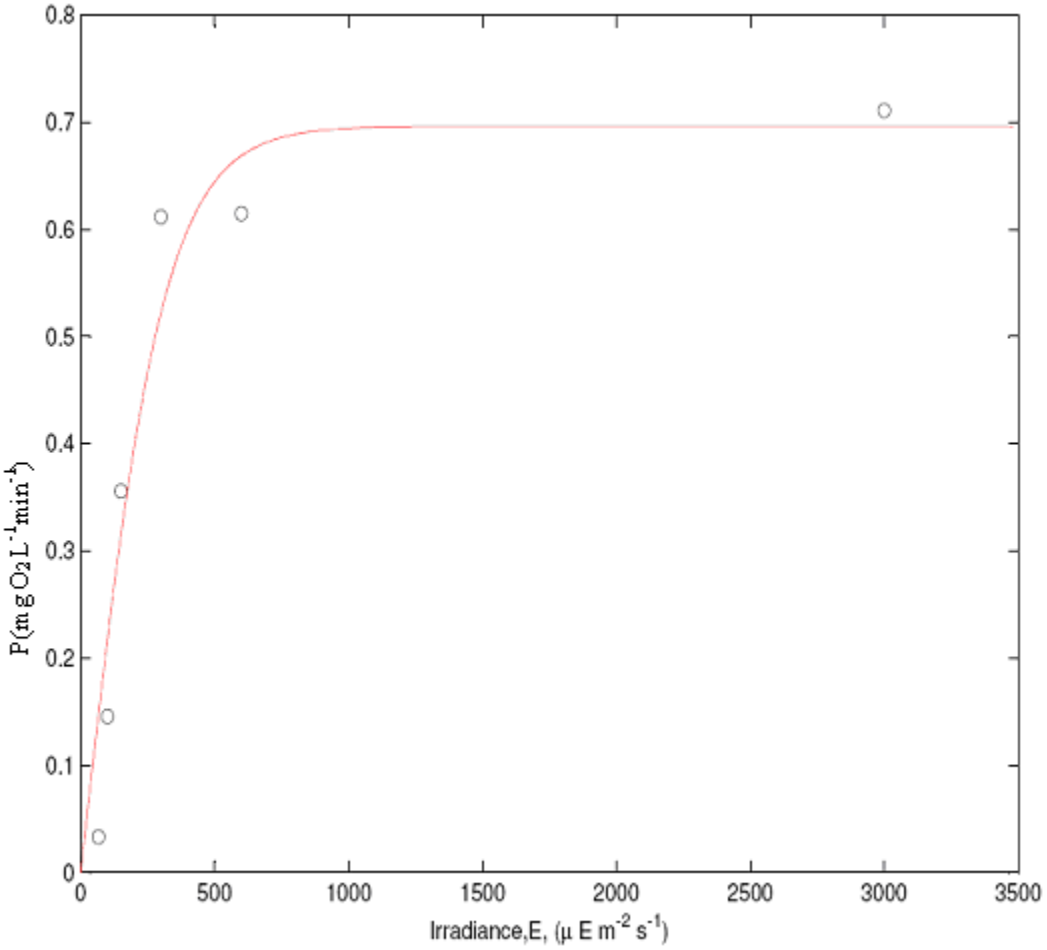

Figure 5.1: Photosynthesis versus irradiance curve obtained from oxygen evolution.

From Fig 5.1 the photosynthetic oxygen production rate increased linearly (0 to 0.6 mg O_2 $L^{-1}min^{-1}$) with irradiance from 0 up to 500 $\mu Em^{-2}s^{-1}$. This region is known as the as light-limited region. The increase in photosynthetic rates in this region is limited by the rate of photon absorbed by the light harvesting antennae. Further increase in irradiance from 500 up to 1000 $\mu Em^{-2}s^{-1}$ led to an increase in photosynthetic rate to from 0.6 mg O_2 $L^{-1}min^{-1}$ towards a saturation level (0.7 mg O_2 $L^{-1}min^{-1}$). At this level the rate of photon absorption exceeds the rate of electron transport in the photosynthesis. This light-saturated region of the graph gives the maximum rate of photosynthesis. At this

maximum photosynthetic rate further increase in irradiance from 1000 $\mu Em^{-2}s^{-1}$ to 3000 $\mu Em^{-2}s^{-1}$ did not result in any increase in photosynthesis. This part of the graph is independent of the light capture processes.

Increasing light beyond the saturation level can lead to the reduction in the photosynthetic rate. This reduction which is dependent on both intensity of light and the duration of exposure is called photoinhibition. Photoinhibition is caused photo-damage in the algae antenna.

5.2 The effect of UVR on algae photosynthesis.

In this part of the chapter we present a few selected results for the inhibition of photosynthesis on algae cells. Photosynthesis (oxygen evolution) was measured in a number of marine and fresh water algae (Table 5.1) for a given period of irradiation of PAR + UVR.

The experiments on the samples were first run in the presence of PAR only for 20 min (0.33 hrs) and thereafter were subjected to both PAR and UVR stress.

Our results show the effects of different UV-B levels (100%, 50% and 20% of the maximum available intensity) on algae photosynthesis under constant levels of UV-A and PAR radiation. These findings clearly show the importance of background PAR for the significance of UV effects.

The effects of experimental exposure under the different radiation conditions are shown in Figures 5.2, 5.3, 5.6, 5.7 and 5.8 shown below.

5.2.1 Inhibition of photosynthesis in *Haematococcus pluvialis* (green algae)

Haematococcus pluvialis is a fresh water species of chlorophyta from the family of Haemotococcaceae. This species is known for its high content of a strong antioxidant and carotenoid pigment astaxanthin. When environment conditions become adverse i.e. when nutrients start becoming scarce, the water environment starts to dry out and algae are increasingly exposed to direct sunlight, they enter a resting phase (cyst phase) which allows them to survive for long prolonged periods until the environment becomes much more favorable for growth and also during this phase algae accumulate a lot of high amounts of astaxanthin that protects them from detrimental effect of UV when exposed to direct sunlight.

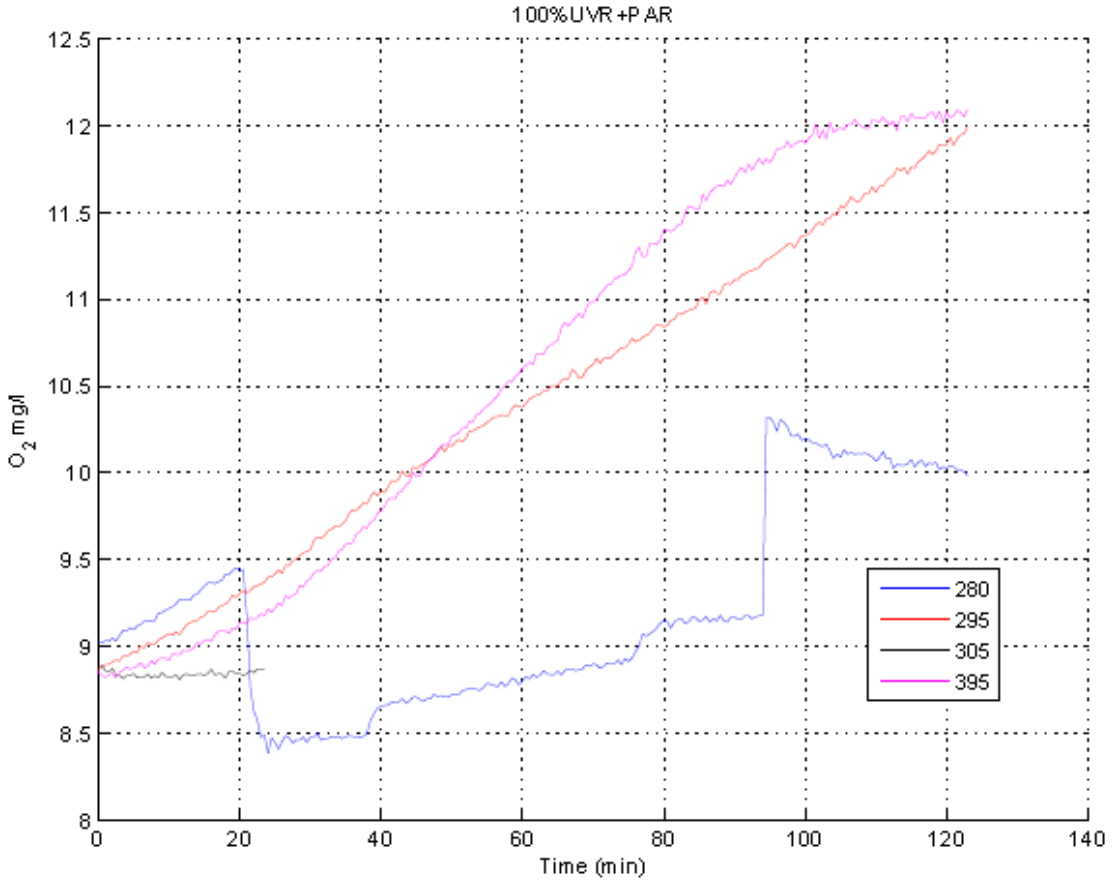

Figure 5.2: The inhibition of algae photosynthesis in *Haematococcus pluvialis* exposed to 100%PAR +UVR. Cut off filters with wavelengths of 280, 295, 305 and 395 nm were used to control the ambient light regime into PAR and PAR+UV

Figure 5.2 illustrate the inhibition of photosynthesis in *Haematococcus pluvialis*. The algae cells were first exposed to PAR only for 20 min; afterwards UVR was then introduced in addition to PAR light. There was a slight increase in oxygen production in the first 20 min in samples with 280, 295 and 395 nm wavelength cut off filters but no increase in graph for samples with 305 nm wavelength cut off filter was observed. When UVR was introduced in addition to PAR, an unrealistic rapid drop in the graph for sample with a 280 nm cut off filter was observed, also followed by an unrealistic rise in the graph at about 95 min. In samples with 295 and 395 nm cut off filters, an increase in oxygen production was observed. After 90 min of exposure to both PAR and UVR unexpected decrease in oxygen production was observed in a 395 nm cut off filter.

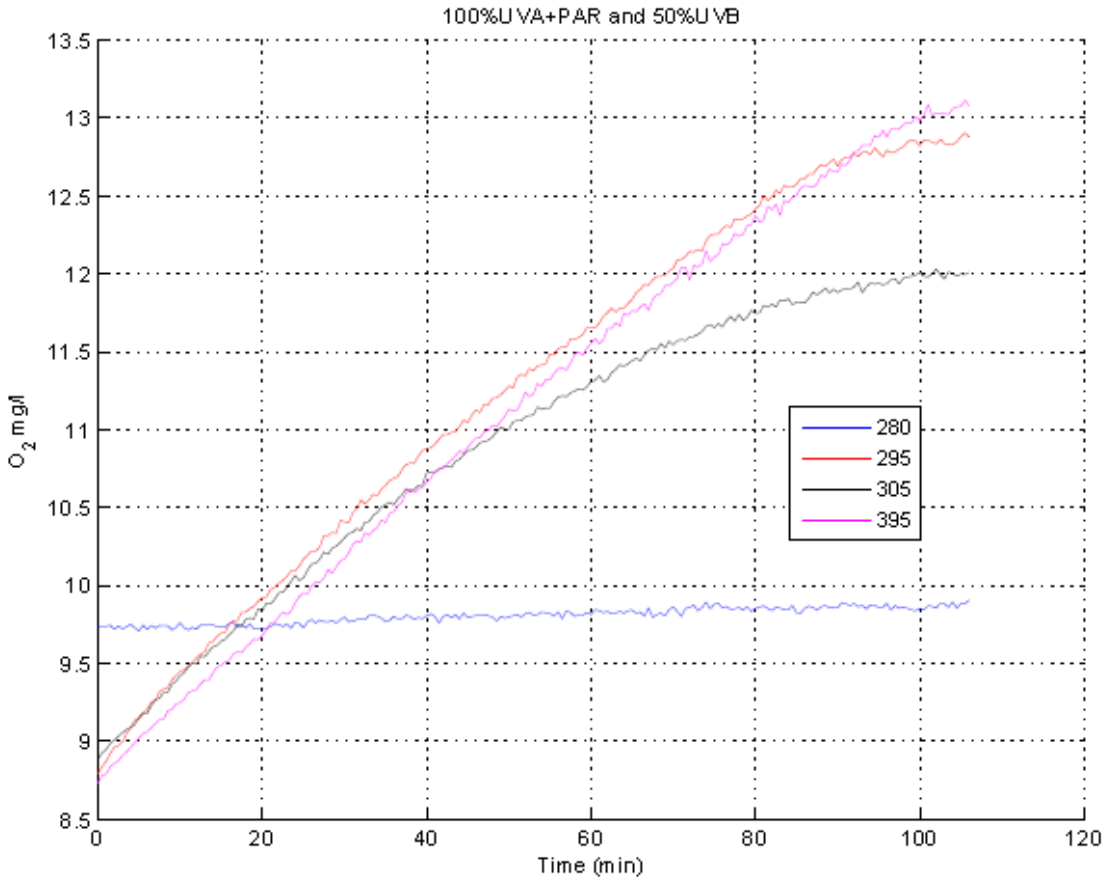

Figure 5.3: The inhibition of algae photosynthesis in *Haematococcus pluvialis* exposed to 100%UVA+PAR and 50%UVR. Cut off filters with wavelengths of 280, 295, 305 and 395 nm were used to control the ambient light regime into PAR and PAR+UV.

Figure 5.3 illustrate the inhibition of photosynthesis in *Haematococcus*. *Pluvialis* exposed to 100 % UVA+PAR and 50 % UVB. The algae cells were first exposed to PAR only for 20 min; afterwards UVR was introduced in addition to PAR. There was a linear increase in oxygen production in the first 50 min of exposure in samples with 295, 305 and 395 nm wavelength cut off filters but no increase in oxygen production was observed in samples with 280 nm wavelength cut off filter. Then a decrease in oxygen production was observed in a sample with a 305 nm cut off after 30min of UVR exposure. In samples with 295 and 395 nm cut off filters, an increase in oxygen production was observed. After 90 min of exposure to both PAR and UVR inhibition of photosynthesis was observed in a 295 nm cut off filter.

Kristin et al 2006 states that the yield in production becomes lower the shorter the wave length and the higher the intensity becomes. However from Figures 5.2 and 5.3 this observation was not successfully achieved. Below are some of the problems faced which are assumed to have affected our results and led to unexpected increase or decrease in either oxygen production or the graphs.

5.2.2 Methodical problems

Formation of air bubbles: When air bubbles are formed on the sensor tip unexpected drifts, gradients or unstable measurement values occur. Critical conditions for bubble formations are for example, purging with air or other gases and increasing temperature during measurements. Increase in temperature was caused by heat from the lamps and the inefficient thermostat that was used to control the water cooler.

Signal drift due to temperature gradients: Temperature gradients were also other source of imprecise measurements. The Oxy-10 meter used, only measures correctly if the sample temperature is constant during measurement and is the same as at the beginning of the experiment.

A lot was done to ensure that these problems were corrected to minimize errors and improve on the results. For example air bubbles were minimized by filling the bottles completely with samples and then sealed using lids.

The problem of the increasing temperature was minimized by replacing the inefficient analog thermostat we were using with a new digital thermostat which was easy to monitor and operate. Below are the temperatures measuring graphs (Figures 5.4-5.5) taken during the experiments that resulted in graphs in Figures 5.2 and 5.3 respectively.

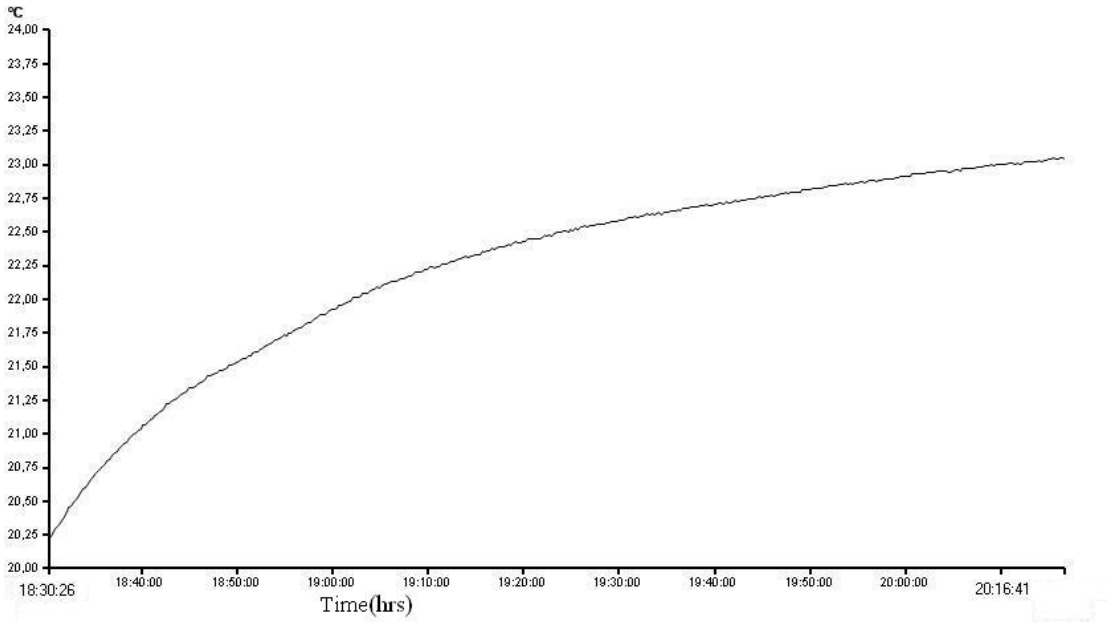

Figure 5.4: The variation of temperature with time as measured using the temperature sensor. This temperature variation was measure during an experiment corresponding to Figure 5.2 before temperature errors were minimized.

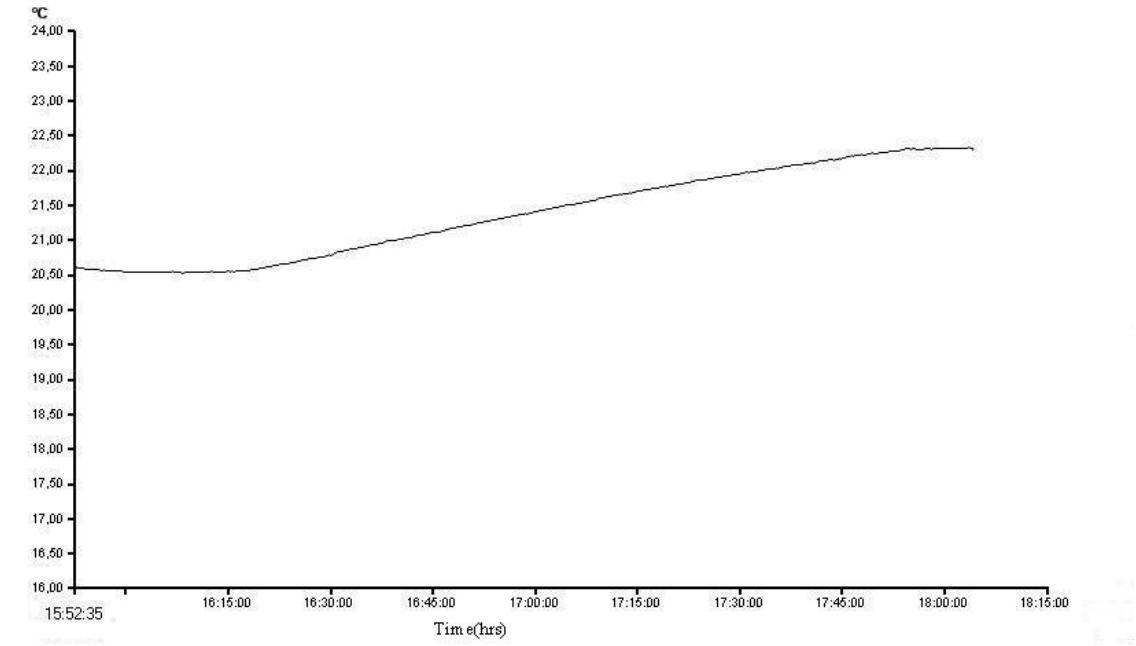

Figure 5.5: The variation of temperature with time as measured using the temperature sensor. This temperature variation was measure during an experiment corresponding to Figure 5.3 after temperature errors were minimized

Signal drift due to photodecomposition: The oxygen-sensitive material may have been subjected to photodecomposition resulting into signal drift. Photodecomposition takes place only during illumination of the sensor tip and depends on the intensity of the excitation light. Therefore the excitation light was minimized. This was done by changing the measuring mode from minutes as in Figures 5.2 and 5.3 shown above to hours as in Figures 5.6, 5.7 and 5.8 shown below.

Although the above expected errors were minimized still there were some irregularities in our results. It was also assumed that either the oxy-10 meter or the oxygen sensors had mechanical problems which we were unable to fix. Some of the expected mechanical problems which are likely to have affected our results included micro bending of the fiber tip (This may affect the oxygen measurements), fading of the black isolating coating that excludes optical interferences from the samples which may be caused by for example scattering effects; chlorophyll fluorescence and others which we couldn't be able to identify.

After the correction of the addressed problems, major improvements were achieved. Below are some improved results achieved on the experiments carried out with *Phaeodactylum tricornutum*.

5.2.3 Inhibition of photosynthesis in *Phaeodactylum tricornutum* (diatom)

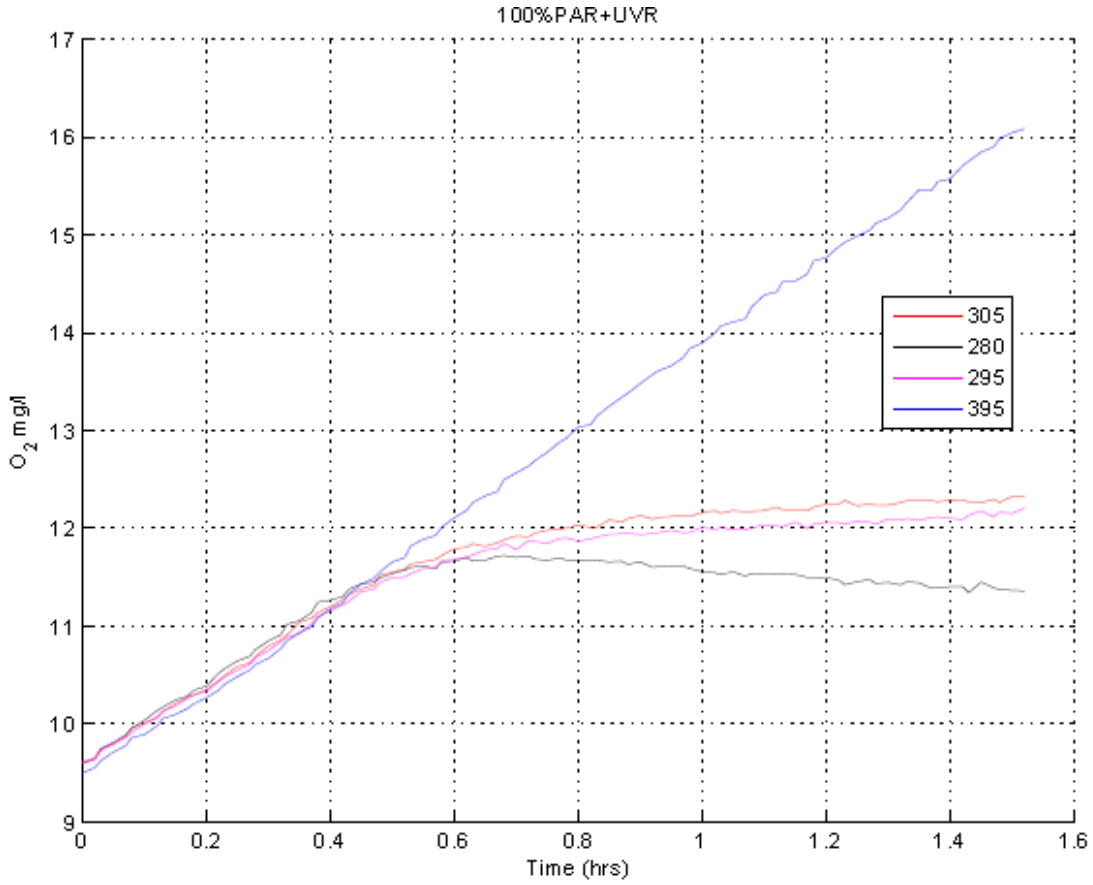

Figure 5.6: The inhibition of algae photosynthesis in *Phaeodactylum tricornutum* exposed to 100%PAR +UVR. Cut off filters with wavelengths of 280, 295, 305 and 395 nm were used to control the ambient light regime into PAR and PAR+UV.

During the period of PAR exposure only (0.33hrs) the photosynthesis in all algae samples (280, 295, 305 and 395) was uninhibited and the increase in oxygen was linear. After a period of 0.17 hrs of exposure of UVR in addition to PAR, four of the algae samples tested (280, 295 and 305) showed a substantial reduction in the oxygen production (inhibition of photosynthesis) relative to the control sample (395 nm) which received only PAR.

The extent and the velocity of inhibition of photosynthesis in the samples tested depended on spectral quality. This is depicted in Figure 5.6 where the shapes of the graphs differ with the changes in the wavelength of the intensity. The effect of UV radiation on the algae oxygen production gradually increased with the decrease in wavelength of light received by the samples. This increase in effect is shown by the decreases in oxygen production in samples with 280 nm, 295 nm and 305 nm cut off filters compared to a 395 nm cut off filter. Strongest inhibition was observed in algae sample with a 280 nm cut off filter followed by algae samples with 295 and 305 nm cut off filters respectively.

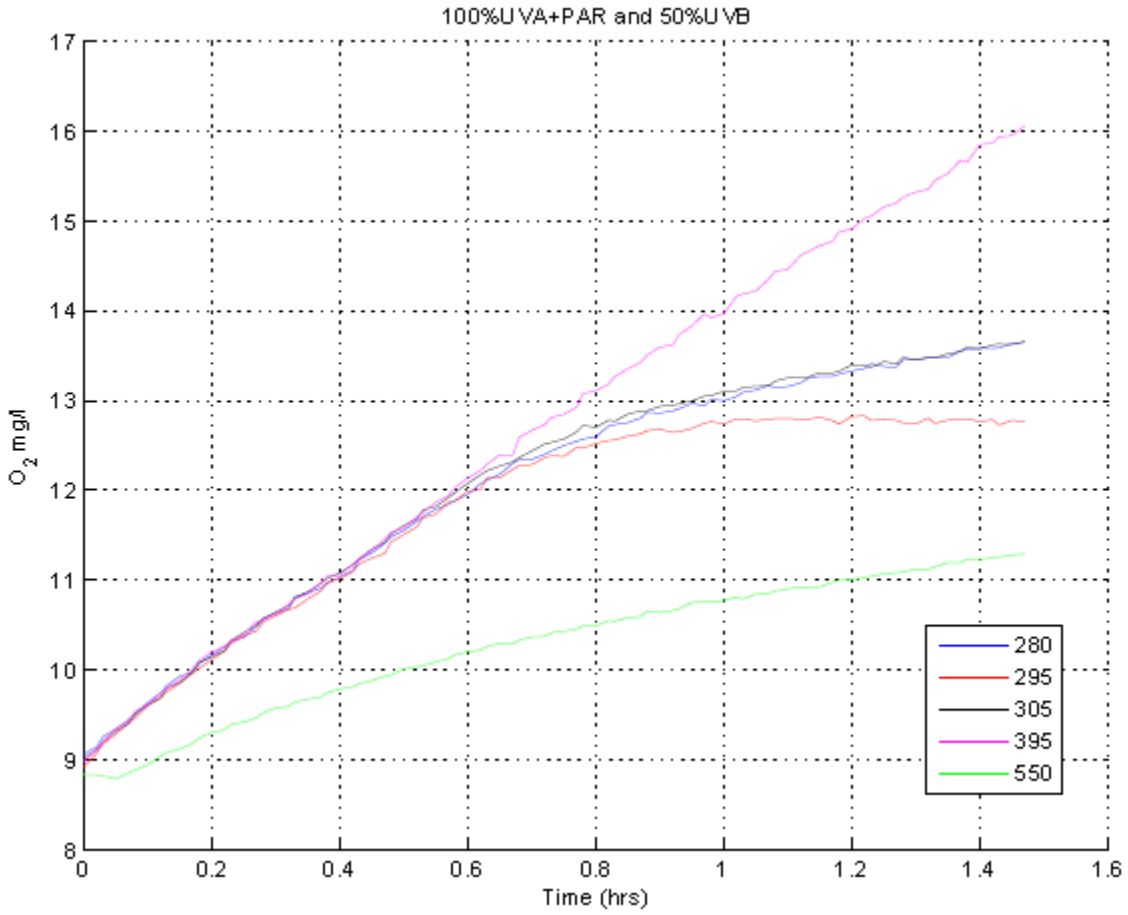

Figure 5.7: The inhibition of algae photosynthesis in *Phaeodactylum tricornutum* exposed to 100%UVA+PAR and 50%UVB. 280, 295, 305 and 395 nm are cut off wavelengths of the filters used to control the ambient light regime into PAR and PAR+UV.

During the period of PAR exposure only (0.33hrs) (Figure.5.7) the photosynthesis in all algae samples (280, 295, 305 and 395) was uninhibited and the increase in oxygen was linear. With 0.27 hrs of exposure of UVR, samples (280 nm, 295, 305 nm) tested started showing a substantial reduction in the oxygen productions relative to the control sample (395 nm) which received only PAR.

The extent of inhibition of photosynthesis in the samples tested depended on the spectral quality with the strongest inhibition in the algae sample with a 280 nm cut off filter which allowed in more light of shorter wavelength. During the exposure of the whole light spectrum (PAB), the effect of UVR radiation on the algae oxygen production increased gradually with the increasing wavelengths of the cut off filters.

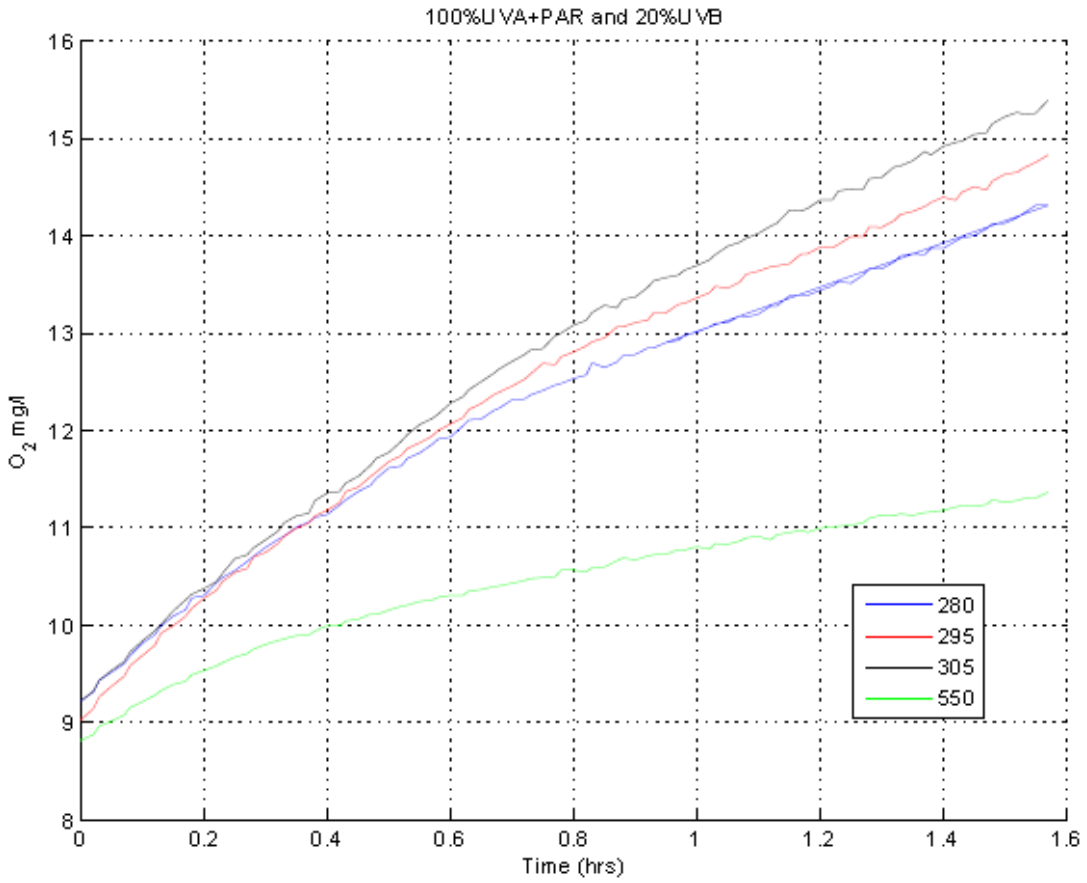

Figure 5.8: The inhibition of algae photosynthesis in Phaeodactylum tricornutum exposed to 100%UVA+PAR and 50%UVB. 280, 295, 305 and 395 are cut off wavelength of the filters used to control the ambient light regime into PAR and PAR+UV.

In Figure 5.8, the photosynthesis measured when algae was first exposed to PAR only (0.33hrs), showed no significant effect. This was shown on the graph by the linear increase in oxygen production with time. A slight reduction in the oxygen production (inhibition of photosynthesis) was observed in all samples when they were exposed to UVR in addition to PAR.

Generally Figures 5.6, 5.7 and 5.8 show that the extent and the velocity of inhibition of photosynthesis in all experiments performed depended on irradiance (UV-B) and spectral quality. This is shown by the shapes of the graphs from the Figures 5.6, 5.7 and 5.8 which vary with the changes in the UV-B intensity (100%, 50% and 20%). The inhibition observed was solely based on UV-induced impairment. Strongest inhibition was observed in algae exposed to the highest UV-B radiation (100%) (Figure.5.6). From Figures 5 6, 5.7 and 5.8, the comparison of the PAR (395 nm cut off filter) and the PAR+UVR (280 nm, 295 nm and 305 nm cut off filters) treatments show the differential contribution of UV-B radiation to the total extent of photoinhibition with the strongest inhibitory contribution of UV-B under the highest (100%) (Figure 5.6) and the weakest share under the lowest irradiance of UV-B (20%) (Figure 5.8).

Photosynthetic rates are clearly associated with the radiation quality under which the cells are exposed. PAR is mostly responsible for photosynthesis, whereas UVR is generally considered a stress factor for the process [83]. However a wide range of responses to UVR is also reported. While some species are resistant, e g. from tropical environments [84] some others e.g. from polar areas are especially sensitive even under low UVR levels [85]. In our studies the PAR applied was low compared to the ambient solar radiation. The relatively higher UVB that was applied induced photoinhibition as found in figures 5.2, 5.3, 5.6, 5.7 and 5.8. Other studies have also repoted the utilization of UVR when PAR levels are low [86].

According to Fredersdorf and Bischof [87], low PAR to UVR ratios often applied in the laboratory studies result in a substantial over estimation of UV effects. This is because in nature high irradiances of UV radiation do only occur in combination with high values of PAR [88].

Fiscus and Booker [89] stated that high UVB exposures at very low PAR levels are necessary to produce the UV effects as those observed in Figures 5.2, 5.3, 5.6, 5.7 and 5.8. Although both UVA and UVB are known to affect photosynthesis, it has been found in our studies that UVB is far more potent in inhibiting photosynthesis and other process.

In order to show the effect of the UVR in the inhibition of the maximum oxygen evolution yield of PSII, the relative inhibition (P_{inh}) values were calculated by subtracting the P_{UVR} respective values of PAB treatments from the PAR treatment as in Equation (4).

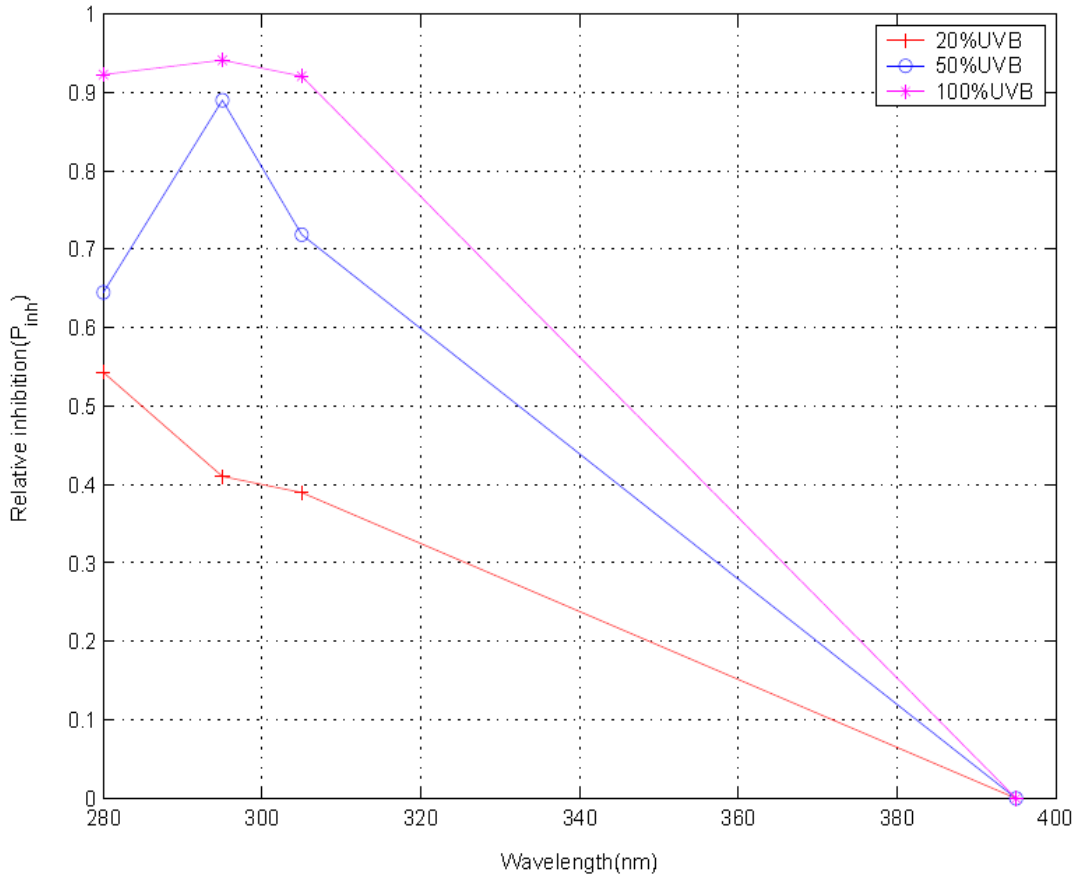

Figure 5.9: The relative inhibition versus wavelength for *Phaeodactylum tricornutum* exposed to different UV-B radiation intensities.

Figure 5.9 demonstrates the contribution of the UVR to the overall inhibition of photosynthesis. The variations seen in the relative inhibition results in the separate experiments were caused by some variations in the UV-B intensities between the experiments. The oxygen evolution yield becomes lower the shorter the wavelength and

the higher the intensity becomes though there was unrealistic decrease in P_{inh} for the 50% UVB graph at 280 nm. This may have been caused by some of the errors already explained. The effect of UVR damage was calculated after the decrease in the oxygen production started to be observed.

6 Conclusion and further research.

In this thesis we successfully developed and implemented an experimental system (the photoinhibitron) for measuring photosynthesis of phytoplankton suspensions during controlled, quantified exposures to broad range of UVR+PAR. The system consists of a water bath which was designed to hold 15 sample bottles in a temperature controlled environment (18-20^{o}). Irradiance was provided by 17 fluorescent lamps. The illumination region was divided into five sections by 5x5 cm long pass filters with nominal cut offs at 280, 295, 305 and 395. The 395 nm long pass filter was used as a control with essentially no UV entering the sample bottle. Our experimental system was found to be appropriate for measuring short term effects of UV radiation on phytoplankton photosynthesis.

We also carried out experiments to evaluate the effects of UVR on phytoplankton photosynthesis. It has been shown in our studies that different levels of UVB inhibit photosynthesis. This is probably due to destruction of photopigments.

This study has shown that treatment of algae for short periods with artificial lights of different levels of UVB, will depress the rate of photosynthesis as measured by oxygen evolution. A higher degree of inhibition was observed in photosynthesis when UVB levels were higher and less inhibition when UVB levels were low.

The phytoplankton cultures investigated in this work were all grown under low light conditions in the absence of UVR. The present results show that *Phaeodactylum tricornutum* was the most sensitive to UVB radiation, in terms of photosynthesis as compared to *Haematococcus pluvialis*. The less sensitivity of *Haematococcus pluvialis* to UVB may probably be due to protective mechanisms or heretofore unrecognized ability to withstand high levels of UVB. Results from other algae species tested were found to be difficult to interpret since the experimental system was still under development and required a lot of improvement to achieve reliable results.

The results from our study indicate that phytoplankton photosynthesis was affected by exposure to UVR, and the apparent effects of UVR clearly depended on the different levels of UVB.

Further studies, however, are needed to compare the oxygen evolution measurements using the fiber optical microsensor with other methods for measuring photosynthetic activity. One of such methods includes the chlorophyll florescence measurements using

the Fast Repetition Rate Fluorometer (FRRF). This instrument has been used in our group for field measurements of primary production. The relationship between these two methods is that both involve measurements which are associated with the photosystem II. Also in our group we have started to do investigations on photosynthetic activity using advanced microscopy technique. In future experiments also this method should be complemented with our inhibitory experiments.

Regarding to the impact of UVR on phytoplankton photosynthesis, more detailed studies are needed to understand the interaction between different environmental variables e.g. increasing temperature, nutrient stress and salinity in the observed effect. Also the impact of UVB on phytoplankton photosynthesis in the field is worthy of more detailed research.

The low PAR to UVR ratios applied in laboratory studies; result in a substantial over estimation of UV effects. Further laboratory studies on UV will therefore need to increase the ecological significance by improving the radiation conditions applied to obtain a ratio of PAR to UVR which is closer to the natural ratios.

A new method of oxygen evolution measurement based on oxygen luminescence quenching in sensor spots was used for the first time to monitor and measure the photosynthetic performance in response to UVB radiation. This method proved to be advantageous in terms of precise and quick oxygen measurements, guarantying the oxygen evolution estimates during a time interval short enough to neglect variations in sample composition, abundance and activity. Therefore we decided to use this technique to quantify the photosynthetic oxygen evolution during our experiments. In spite of some problems faced, we believe that if corrected, the sensors would also be useful for future field work.

References

1. XiangCheng.Y., et al., Effects of ultraviolet radiation B (UV-B) on photosynthesisof natural phytoplankton assemblages in a marine bay in Southern China. Chinese Science Bulletin, 2007. **52**(4): p. 545-552.
2. http://www.ccpo.odu.edu/SEES/ozone/oz_class.htm.
3. Hargreaves.B.R., Water column optics and penetration of UVR. In UV Effects in Aquatic Organisms and Ecosystems (Edited by E. W. Helbling and H. Zagarese). 2003: p. 59–105. The Royal Society of Chemistry, Cambridge.
4. Tedetti.M. and Sempe´re´.R., Penetration of Ultraviolet Radiation in the Marine Environment. Photochemistry and Photobiology, 2006. **82**( ): p. 389–397.
5. Kirk.J.T.O, Light and Photosynthesis in the Aquatic Environment.2nd Edn, Cambridge University Press, Cambridge. Krause GH (1988) Photoinhibition of photosynthesis. An evaluation of damaging and photoprotective mechanisms. Physiol. Plant, 1994. **74**: p. 566–574.
6. Hanelt.D., et al., Light regime in an Arctic fjord: a study related to stratospheric ozone depletion as a basis for determination of UV effects on algal growth. Marine Biology, 2001. **138**: p. 649-658.
7. Farman.J.C., Gardiner.B.G., and J.D. Shanklin, Large losses of total ozone in Antarctica reveal seasonal ClOxNOx interaction. Nature, 1985. **315**( ): p. 207-10.
8. Smith.R.C., et al., Ozone depletion: ultraviolet radiation and phytoplankton biology in Antarctic waters. Science, 1992. **255**: p. 952-959.
9. Piazena.H. and Häder.D.P, Penetration of solar UV and PAR into different waters of the Baltic Sea and remote sensing of phytoplankton. In: Häder DP (ed) The effect of ozone depletion on aquatic ecosystems, R.G. Landes Company, Academic Press, Austin. 1997: p. 45-96.
10. Hader.D-P., et al., Effects on aquatic ecosystems. Journal of Photochemistry and Photobiology B: Biology, 1998. **46**( ): p. 53-68.
11. Häder D-P., et al., Effects of increased solar UV-B radiation on aquatic ecosystems. In: United Nations Environment Programme (UNEP) International

Committee on Effects of Ozone Depletion, UNEP Report on the Environmental Effects of Ozone Depletion. 1994: p. 65-77. ISBN 92 807 1457 0.

12. Karentz., Cleaver.J.E., and Mitchell.D.L, Cell survival characteristics and molecular responses of Antarctic phytoplankton to ultraiolet-b radiation. J Phycol, 1991. **27**: p. 326-341.

13. Ignatides.L, Photosynthetic capacity of the surface microlayer during the mixing period. J. Planktonic Res., 1990. **12**: p. 851-860.

14. D.P.Hader., et al., Effects on aquatic ecosystems. Journal of Photochemistry and Photobiology B: Biology, 1998. **46**: p. 53-68.

15. Crumpton.W.G. and Wetzel.R.G, Effects of differential growth and mortality in the seasonal succession of phytoplankton populations in Lawrence Lake, Michigan. Ecology 1982. **63**( ): p. 1723-1739.

16. Williamson.P. and T.Platt, Ocean Biogeochemistry and Air-Sea CO2 Exchange. Global Change IGPB Newsletter. 1991. **7**: p. 3-4.

17. Häder.D.P., R.C.Worrest., and H.D.Kumar, Aquatic ecosystems. Chapter 4 in Environmental effects of ozone depletion: 1991 update. Nairobi: United Nations Environment Programme. 1991.

18. R.D.Rundel, Action spectra and estimation of biologically effective UV radiation. Physiol. Plant, 1983. **58**: p. 360–366.

19. Falkowski.P.G, Light-shade adaptation in marine phytoplankton. Pages 99-117 in P. G. Falkowski, ed. Primary productivity in the sea. Plenum, New York. 1980.

20. Lewis.M.R., et al., Turbulent motions may control phytoplankton photosynthesis in the upper ocean. Nature, 1984. **311**: p. 49-50.

21. Bühlmann.B., Bossard.P., and Uehlinger.U, The influence of longwave ultraviolet radiation (u.v.-A) on the photosynthetic activity (14C assimilation) of phytoplankton. J Plankton Res, 1987. **9**: p. 935-943.

22. Cullen.J.J. and Lesser.M.P, Inhibition of photosynthesis by ultraviolet radiation as a function of dose and dosage rate: results for a marine diatom. Mar Biol 1991. **111**: p. 183-190.

23. Villafañe.V.E., et al., Inhibition of phytoplankton photosynthesis by solar ultraviolet radiation: Studies in Lake Titicaca, Bolivia. Freshwat Bio, 1999. **l 42**: p. 215-224.

24. Aalderink.R.H. and Jovin.R, Estimation of the photosynthesis / irradiance (P/I) curve parameters from light and dark bottle experiments. J Plankton Res, 1997. **19**: p. 1713-1742.

25. Steemann.Nielsen.E, The use of radio-active carbon (C14) for measuring organic production in the sea. J Cons Perm Int Explor Mer 1952. **18**: p. 117-140.

26. Helbling.E.W., et al., Impact of natural ultraviolet radiation on rates of photosynthesis and on specific marine phytoplankton species. Mar Ecol Prog Ser, 1992b. **80**: p. 89-100

27. Revsbech.N.P, An oxygen microelectrode with a guard cathode. Limnol Oceanogr, 1989. **34**: p. 474-478.

28. Sundbäck.K., et al., Does present UV-B radiation influence marine diatom-dominated microbial mats? A case study. Aquat Microb Ecol, 1996. **11**: p. 151-159.

29. Sundbäck .K., et al., Effects of UV-B radiation on a marine benthic diatom mat. Mar Biol, 1997. **128**: p. 171-179.

30. Garcia-Pichel.F. and Bebout.B.M, Penetration of ultraviolet radiation into shallow water sediments: High exposure for photosynthetic communities. Mar Ecol Prog Ser 1996. **131**: p. 257-262.

31. Henley.W.J., et al., Diurnal responses of photosynthesis and fluorescence in Ulva rotundata acclimated to sun and shade in outdoor culture. Mar Ecol Prog Ser, 1991. **75**: p. 19-28.

32. Schreiber.U., et al., Quenching analysis of chlorophyll fluorescence by the saturation pulse method: Particular aspects relating to the study of eukaryotic algae and cyanobacteria. Plant Cell Physiol, 1995. **36**: p. 873-882.

33. Schreiber.U., Schliwa.U., and Bilger.W, Continuous recording of photochemical and non-photochemical chlorophyll fluorescence quenching with a new type of modulation fluorometer. Photosynt Res, 1986. **10**: p. 51–62.

34. Genty.B., Briantais.J., and Baker.N.R, The relationship between the quantum yield of photosynthetic electron transport and quenching of chlorophyll fluorescence. Biochim Biophys Acta, 1989. **990**: p. 87-92.

35. Flameling.I.A. and Kromkamp.J, Light dependence of quantum yields for PSII charge separation and oxygen evolution in eukaryotic algae. Limnol Oceanogr, 1998. **43**: p. 284-297.

36. Dodds.W.K., Biggs.B.J.F., and Lowe.R.L, PHOTOSYNTHESIS-IRRADIANCE PATTERNS IN BENTHIC MICROALGAE: VARIATIONS AS A FUNCTION OF ASSEMBLAGE THICKNESS AND COMMUNITY STRUCTURE. J. Phycol, 1999. **35**: p. 42–53.

37. Kühl.M., et al., Photosynthetic performance of surface-associated algae below sea ice as measured with a pulse-amplitude-modulated (PAM) fluorometer and O2 microsensors. MARINE ECOLOGY PROGRESS SERIES Mar Ecol Prog Ser, 2001. **223**: p. 1–14.

38. Leech.D.M. and Johnsen.S, Behavioral responsen – UVR avoidance and vision. In: Helbling EW, Zagarese HE (eds) UV effects in aquatic organisms and ecosystems, Comprehensive Series in Photochemical and Photobiological Sciences, The Royal Society of Chemistry, Cambridge. 2003: p. 455-481.

39. Williamson.C.E. and Zagarese.H.E, UVR effects on aquatic ecosystems: a changing climate perspective. In: Helbling EW, Zagarese HE (eds) UV effects in aquatic organisms and ecosystems, Comprehensive Series in Photochemical and Photobiological Sciences, The Royal Society of Chemistry, Cambridge. 2003: p. 547-567.

40. Lancelot.C, Factors affecting phytoplankton extracellular release in the Southern Bight of the North Sea. Ecol. Prog. Ser., 1983. **12**: p. 115-121.

41. Takahashi.M., Fujii.K., and Parsons.T.R, Simulation Study of Phytoplankton Photosynthesis and Growth in the Fraser River Estuary Marine Biology, 1973. **19**: p. 102--116.

42. Gilmore.A.M. and Govindjee., How higher plants respond to excess light: Energy dissipation in Photosystem II. Narosa Publishers/Kluwer Academic Publishers, 1999: p. 513–548.

43. Volkov.A.G., et al., Light energy conversion with chlorophyll a and pheophytin a monolayers at the optically transparent SnO2 electrode:artificial photosynthesis. Bioelectroehemistry and Bioenergetics, 1995. **38**: p. 333-342.

44. Hewes.C.D., G.M.B., et al., THE PHYCOBILIN SIGNATURES OF CHLOROPLASTS FROM THREE DINOFLAGELLATE SPECIES: A MICROANALYTICAL STUDY OF DINOPHYSIS CAUDATA, D. FORTII, AND D. ACUMINATA (DINOPHYSIALES, DINOPHYCEAE). J. Phycol, 1998. **34**: p. 945–951.

45. OKADA.M. and TAKAMIYA.A, Light-induced absorption spectrum changes of carotenoid in chromatophores of photosynthetic bacterium, Rhodopseudomonas spheroides II. Rapid and slow absorption changes of carotenoid in chromatophores. Plant & Cell Physiol, 1971. **12**: p. 683-694.

46. http://www.bio.umass.edu/biology/conn.river/misc_images/photosyn4.jpg.

47. Falkowski.P.G. and J.A.Raven, Aquatic photosynthesis. Second edition, princeton university press, New Jersey. 2007.

48. Falkowski.P.G and J.A. Raven, Aquatic Photosynthesis. Blackwell Science, Oxford, UK. 1997. **375**.

49. Hoganson.C.W. and Babcock.G.T., A Metalloradical Mechanism for the Generation of Oxygen from Water in Photosynthesis. Science, 1997. **277**: p. 1953-1956.

50. Haumann.M., et al., Photosynthetic O2 Formation Tracked by Time-Resolved X-ray Experiments. Science, 2005. **310**: p. 1019-1021.

51. Vass.I, Adverse effects of UV-B light on the structure and function of the photosynthetic apparatus. In: Handbook of Photosynthesis. Pessarakli M (ed). Marcel Dekker Inc. New York:. 1997: p. 931-949.

52. Bischof.K, Hanelt.D, and Wiencke.C., Effects of ultraviolet radiation on photosynthesis and related enzyme reactions of marine macroalgae. Planta, 2000. **211**: p. 555-562.

53. Greenberg.B..M., et al., Separate photosensitizers mediate degradation of the 32-kDa photosystem II reaction centre protein in the visible and UV spectral regions. Proc. Natl. Acad. Sci. U S A, 1989. **86**: p. 6617–6620.

54. Melis.A., J. A.Nemson., and M. A.Harrison, Damage to the functional components and partial degradation of photosystem II reaction center proteins upon

chloroplast exposure to ultraviolet B radiation. Biochim. Biophys. Acta, 1992. **1100**: p. 312–320.

55. Prasil.O., N.Adir., and I.Ohad, Dynamics of photosystem II:Mechanism of photoinhibition and recovery processes. In The Photosystems: Structure, Function and Molecular Biology (Edited by J. Barber). Elsevier Science Publishers, New York., 1992: p. 295–348.

56. Mulo.P., et al., Stepwise photoinhibition of photosystem II. Plant Physiol, 1998. **117**: p. 483–490.

57. Aro.E.-M., I.Virgin., and B.Andersson, Photoinhibition of photosystem II: Inactivation, protein damage and turnover. Biochim.Biophys. Acta, 1993. **1143**: p. 113–134.

58. Vass.I., et al., Reversible and irreversible intermediates during photoinhibition of photosystem II: Stable reduced QA species promote chlorophyll triplet formation. Proc. Natl. Acad. Sci. U S A, 1992. **89**: p. 1408–1412.

59. Blaubaugh.D.J. and G.M.Cheniae, Kinetics of photoinhibition in hydroxylamide-extracted photosystem II membranes—Relevance to photoactivation and sites of electron donation. 29, 1990. **Biochem**: p. 5109–5118.

60. Tyystjärvi.E, Photoinhibition of Photosystem II and photodamage of the oxygen evolving manganese cluster. 2008. **252**: p. 361–376.

61. Lois.R. and Buchanan, Severe sensitivity to ultraviolet radiation in an Arabidopsis mutant deficient in flavonoid accumulation: II. Mechanisms of UVresistance in Arabidopsis. Planta, 1994. **194**: p. 504-509.

62. Strid.A., Chow.W.S., and Anderson.J.M, Effects of supplementary ultraviolet-B radiation on photosynthesis in Pisum sativum. Biochimica et Biophysica Acta, 1990. **1020**: p. 260-268.

63. Roleda.M.Y., Wiencke.C., and Hanelt.D, Thallus morphology and optical characteristics affect growth and DNA damage by UV radiation in juvenile Arctic Laminaria sporophytes. Planta, 2006a. **223**: p. 407-417.

64. Roy.S, Strategies for the minimization of UV-induced damage. In: De Mora S, Demers S,Vernet M (eds) The effects of UV radiation in the marine environment.

Cambridge Environ Chem Ser 10, Cambridge University Press, Cambridge. 2000: p. 177-205.

65. Tilzer.M.M, Diurnal periodicity in the phytoplankton assemblage of a high mountain lake. Limnol Oceanogr, 1973. **18**: p. 15-30.

66. Hoyer.K., et al., Photoprotective substances in Antarctic macroalgae and their variation with respect to depth distribution, different tissues and developmental stages. Mar Ecol Prog Ser, 2001. **211**: p. 117-129.

67. Bandaranayakie.W.M, Mycosporines: are they nuture's sunscreens? Nat prod Res, 1998. **15**: p. 159-172.

68. Neale.P.J., Banaszak.A.T., and Jarriel.C.R, Ultraviolet sunscreens in Gymnodinium sanguineum (Dinophyceae): Mycosporine-like amino acids protect against inhibition of photosynthesis. J.Phycol, 1998a. **34**: p. 928-938.

69. Banaszak.A.T, Photoprotective physiological and biochemical responses of aquatic organisms. In: Helbling EW, Zagarese HE (eds) UV effects in aquatic organisms and ecosystems, Comprehensive Series in Photochemical and Photobiological Sciences. The Royal Society of Chemistry, Cambridge, 2003: p. 329-356.

70. Underwood.G.J.C., et al., Short-term effects of UV-B radiation on chlorophyll fluorescence, biomass, pigments, and carbohydrate fractions in a benthic diatom mat. J Phycol, 1999. **35**: p. 656-666.

71. Buma.A.G.J., Engelen.A.H., and Gieskes.W.W.C, Wavelength-dependent induction of thymine dimers and growth rate reduction in the marine diatom Cyclotella sp. exposed to ultraviolet radiation. Mar Ecol Prog Ser, 1997. **153**: p. 91-97.

72. Buma.A.G.J., Boelen.P., and Jeffrey.W.H, UVR- induced DNA damage in aquatic organisms. In: Helbling EW, Zagarese HE (eds) UV effects in aquatic organisms and ecosystems, Comprehensive Series in Photochemical and Photobiological Sciences, The Royal Society of Chemistry, Cambridge. 2003: p. 291—327.

73. Mitchell.D.L. and Karentz.D, The induction and repair of DNA photodamage in the environment. In: Young AR, Björn LO, Moan J, Nultsch W (eds) Environmental UV Photobiology, Plenum Press, New York. 1993: p. 345-377.

74. Villafañe.V.E., et al., Acclimatization of Antarctic natural phytoplankton assemblages when exposed to solar ultraviolet radiation. J Plankton Res, 1995b. **17**: p. 2295-2306.

75. Klimant., et al., Optical measurement of oxygen temperature in microscale: strategies and biological applications. Sensors and Actuators, 1997: p. 29-37.

76. Warkentin.M., et al., New and Fast Method To Quantify Respiration Rates of Bacterial and Plankton Communities in Freshwater Ecosystems by Using Optical Oxygen Sensor Spots. APPLIED AND ENVIRONMENTAL MICROBIOLOGY, 2007. **73**: p. 6722–6729.

77. 10-Channel Fiber-Optical Oxygen Meter (OXY-10) Instruction mannual. 2005.

78. THAR.R., KUHL.M., and HOLST.G, Fiber-Optic Fluorometer for Microscale Mapping of Photosynthetic Pigments in Microbial Communities. APPLIED AND ENVIRONMENTAL MICROBIOLOGY, 2001. **67**: p. 2823–2828.

79. Kautsky.H., Quentching of luminescence by oxygen. Trans. Farad. Soc, 1939. **35**: p. 216.

80. McDonagha.C., et al., Phase fluorometric dissolved oxygen sensor. Sensors and Actuators, 2001. **74**(B): p. 124-130.

81. Klimant.I., Holst.G., and Kuhl.M, A Simple Fiberoptic Sensor to Detect the Penetration of Microsensors Into Sediments and Other Biogeochemical Systems. Limnology and Oceanography, 1997. **42**: p. 1638-1643.

82. Klimant.I., V.Meyer., and M.Kuhl, Fiber-optic oxygen microsensors, a new tool in aquatic biology. Limnol. Oceanogr, 1995. **40**: p. 1159–1165.

83. Villafañe.V.E., et al., Photosynthesis in the aquatic environment as affected by UVR. In: E.W. Helbling & H.E. Zagarese (eds.). UV effects in aquatic organisms and ecosystems. The Royal Society of Chemistry, Cambridge. 2003: p. 357-397.

84. Helbling.E.W., et al., Impact of natural ultraviolet radiation on rates of photosynthesis and on specific marine phytoplankton species. Mar. Ecol. Progr.Ser, 1992. **80**: p. 89-100.

85. Helbling.E.W., et al., Effects of ultraviolet radiation on post-bloom phytoplankton populations in Kvalsund, North Norway. J. Photochem. Photobiol., B-Biol, 1996. **33**: p. 255-259.

86. Barbieri.E.S., V.E.Villafañe., and E.W.Helbling., Experimental assessment of UV effects on temperate marine phytoplankton when exposed to variable radiation regimes. Limnol. Oceanogr, 2002. **47**: p. 1648-1655.

87. Fredersdorf.J. and Bischof.K, Irradiance of photosynthetically active radiation determines ultraviolet-susceptibility of photosynthesis in Ulva lactuca L. (Chlorophyta). Phycological Research, 2007. **55**: p. 295–301.

88. Hanelt.D., Wiencke.C., and Bischof.K, Photosynthesis in marine Macroalgae. In Larkum, A. W., Douglas, S. E. and Raven, J. A. (Eds) Photosynthesis in Algae. Advances in Photosynthesis and Respiration 18. Kluwer Acedemic Publishers, Dordrecht. 2003: p. 413–35.

89. Fiscus.E.L. and Booker.F.L, Is increased UV-B a threat to crop photosynthesis and productivity? Photosynth. Res, 1995. **43**: p. 81–92.